

VESTIBULAR CONNECTIVITY TO SOLEUS MOTOR UNITS
DURING QUIET STANCE

by

GREGORY MARTIN LEE SON

B.Sc., The University of British Columbia, 2003

A THESIS SUBMITTED IN PARTIAL FULFILLMENT OF
THE REQUIREMENTS FOR THE DEGREE OF

MASTER OF SCIENCE

in

THE FACULTY OF GRADUATE STUDIES

(Human Kinetics)

THE UNIVERSITY OF BRITISH COLUMBIA

April 2007

© Gregory Martin Lee Son, 2007

Abstract

Galvanic vestibular stimulation (GVS) applied to humans engaged in a postural task evokes a distinct biphasic response in the soleus muscle. The purpose of this study was to investigate vestibular connectivity to individual soleus motor units in quiet standing humans. Subjects were instructed to stand quietly with their heads facing forward, eyes open, and feet together. GVS perturbations (4 mA, 30 msec pulses) were delivered bilaterally to the mastoid processes in a bipolar, binaural configuration. Surface and intramuscular wire electromyography (EMG) were recorded from the right soleus muscle. Surface EMG responses were trigger-averaged to the onset of the GVS pulse and quantified by determining onset latencies, peak-to-peak amplitudes, and peak latencies. Single motor units were identified using a template-matching algorithm. Post-stimulus time histograms (PSTHs) were created for each motor unit using GVS as the trigger (time = 0). PSTHs were analyzed using 2 msec bins to determine the number of occurrences the motor unit fired at specific post-trigger latencies. Individual motor unit responses to GVS differed between various units recorded in soleus. Certain motor units were influenced by GVS and exhibited a characteristic biphasic response in their PSTH at latencies of ~80 and ~120 msec. In contrast, other motor units were not influenced by GVS and therefore exhibited a constant probability of firing. Motor unit triggered-averages (MUTAs) were created from trigger-averaging the surface EMGs to the onset of the individual motor unit firing. Motor units that were influenced by the descending vestibular volley produced MUTAs that were 1.6x greater in peak-to-peak amplitude than the non-influenced motor units. The observations suggest that in humans, vestibular input projects non-uniformly on the soleus motoneuron pool with a bias towards higher threshold motor units.

TABLE OF CONTENTS

<u>TITLE</u>	<u>PAGE</u>
Abstract.....	ii
Table of Contents.....	iii
List of Tables.....	v
List of Figures.....	vi
Acknowledgements.....	viii
Introduction.....	1
Materials and Methods.....	5
• Participants.....	5
• Electromyography.....	5
• Galvanic Vestibular Stimulation.....	7
• Experimental Task and Design.....	8
• Data Analyses and Statistics.....	9
Results.....	12
• GVS-Evoked Muscle Responses.....	13
• Motor Units.....	19
• Motor Unit Classification.....	25
Discussion.....	28
References.....	35
Appendix A: Literature Review.....	41
• Vestibular System.....	42
• Galvanic Vestibular Stimulation.....	45

- GVS Vector Model 47
- GVS-Evoked Muscle Responses 48
- Motor Units 56
- Intramuscular Wire Electrodes 59
- Template-Matching..... 61
- Appendix B: UBC Research Ethics Board Certificate of Approval 63
 - Clinical Research Ethics Board: Certificate of Full Board Approval..... 64

LIST OF TABLES

<u>TITLE</u>	<u>PAGE</u>
Table 1. Number of motor units collected from each wire electrode for each subject	12
Table 2. Individual and mean onset latencies from the GVS-evoked soleus responses recorded from lateral and medial surface EMG	16
Table 3. Individual and mean peak-to-peak amplitudes from the GVS-evoked soleus responses recorded from lateral and medial surface EMG.....	17
Table 4. Individual and mean peak latencies from the GVS-evoked soleus responses recorded from lateral and medial surface EMG	18
Table 5. R values, PSTH significance scores, and normalized MUTA peak-to-peak amplitudes for R-Low motor units.....	23
Table 6. R values, PSTH significance scores, and normalized MUTA peak-to-peak amplitudes for R-High motor units.....	24

LIST OF FIGURES

<u>TITLE</u>	<u>PAGE</u>
Figure 1. Hypothetical and actual surface electrode placements and intramuscular wire insertions.....	7
Figure 2. GVS electrode configurations.....	9
Figure 3. Raw data recorded from GVS, surface EMG from the right soleus, and intramuscular EMG from the right soleus	14
Figure 4. GVS-evoked muscle responses recorded from the medial and lateral soleus averaged over all subjects	15
Figure 5. Raw intramuscular EMG and three template-matched motor units.....	20
Figure 6. PSTHs for the anode right and cathode right GVS configurations from a single motor unit that is affected by GVS	21
Figure 7. PSTHs for the anode right and cathode right GVS configurations from a single motor unit that is not affected by GVS	22
Figure 8. Correlated r values from all identified motor units plotted against their PSTH significance score.....	26
Figure 9. Mean PSTH significance scores and normalized MUTA peak-to-peak amplitudes for R-Low and R-High motor units	27
Figure 10. Schematic drawing of pathways that interact with the vestibular nuclei.....	45
Figure 11. GVS-evoked muscle responses in the lower limb muscles	51
Figure 12. Modulation of GVS-evoked muscle responses in soleus based on background EMG.....	53

Figure 13.	Modulation of GVS-evoked muscle responses in tibialis anterior based on CoM	54
Figure 14.	Recruitment of motor units from the right soleus when torque output is increased step-wise to 20% MVC	58
Figure 15.	Motor unit triggered-averages from two motor units	59
Figure 16.	Intramuscular wire electrodes	60

Acknowledgements

First and foremost, I would like to thank my supervisor, Dr. Timothy Inglis, for his support throughout the project. Thank you for giving me a chance to become involved in the world of research. Also, thanks to my committee members, Drs. Mark Carpenter and Tania Lam, for their insight and comments over that last year. A very special thanks to Dr. Jean-Sébastien Blouin who has provided guidance and advice throughout my entire Masters program. This project would not have been possible without your help. Thank you to my labmates, Dr. Paul Kennedy, Chris Dakin, Brynne Elliott, Dave Nichol, and Melanie Roskell who provided support and allowed me to pilot my study numerous times on them. I would also like to thank all of the people who participated in my experiment. On a personal note, Kirstin, you were the one to push me and I am glad we shared our Masters' experiences together; you have definitely become one of my idols. Finally, I would like to thank my Mom, Dad, and Nicole for the support they have given me throughout my academic career. Thank you for giving me this opportunity to explore myself.

Introduction

The role of vestibular information during quiet stance remains a subject of continued debate, as research evidence suggests vision and somatosensory inputs appear to be the dominant sources of afferent information¹ (Peterka and Benolken 1995). Although the role of vestibular information in quiet stance is debatable, many researchers have probed the vestibular system using galvanic vestibular stimulation (GVS) during quiet stance to investigate possible postural and muscular responses² (Nashner and Wolfson 1974; Iles and Pisini 1992; Britton et al. 1993; Fitzpatrick et al. 1994; Inglis et al. 1995; Watson and Colebatch 1997; Pavlik et al. 1999; Fitzpatrick and Day 2004). In a bilateral, bipolar configuration, GVS delivers a current percutaneously to the vestibular system such that it alters the firing rates of the vestibular afferents. This GVS configuration decreases the firing rates of the afferents under the anode and increases the firing rates of the afferents under the cathode (Goldberg et al. 1984; Minor and Goldberg 1991) with a preferential bias toward the irregular afferents (Goldberg 2000). The error signal resulting from this pure vestibular perturbation produces virtual roll and yaw movements toward the side of the cathode³ (Fitzpatrick and Day 2004). Therefore, it is thought that the body responds with whole-body postural responses of movements toward the side of the anode (Lund and Broberg 1983; Pastor et al. 1993). Muscles that are engaged in a postural task when GVS is delivered exhibit well-defined responses present in the recorded surface electromyography (EMG)⁴ (Britton et al. 1993; Fitzpatrick et al. 1994; Lee Son et al. 2005). In contrast, it remains unclear how vestibular signals acting

¹ For more information on the vestibular system, see Appendix A: Vestibular System

² For more information on galvanic vestibular stimulation, see Appendix A: Galvanic Vestibular Stimulation

³ For more information on the GVS vector model, see Appendix A: GVS Vector Model

⁴ For more information on GVS-evoked muscle responses, see Appendix A: GVS-Evoked Muscle Responses

on the spinal cord interact with individual motor units from muscles engaged in a postural task such as quiet stance⁵.

GVS-evoked muscle responses were modulated by stimulation parameters (Britton et al. 1993; Fitzpatrick et al. 1994), changes in visual and somatosensory input (Britton et al. 1993), position of the centre of mass (Lee Son et al. 2005), and background muscle activity (Lee Son et al. 2005). GVS-evoked muscle responses in soleus and tibialis anterior increased in peak-to-peak amplitude when background EMG increased (Lee Son et al. 2005). This observation could be a consequence of stronger vestibular connections with higher threshold motor units recruited during periods of greater background muscle activity. It is possible that the input-output function between vestibular signals on the spinal cord and motoneuron pools is not uniform. In fact, it is probable that vestibular input has a greater influence on higher threshold motor units and that these motor units are responsible for the GVS-evoked muscle responses seen in surface EMG.

Differential afferent inputs to motor units have been observed previously for other afferent systems in both cats and humans. In the cat, cutaneous afferents projected differently to triceps surae motor units. Electrical stimulation to the sural nerve in cats produced inhibitory post-synaptic potentials in small, low-threshold motor units and excitatory post-synaptic potentials in large, high-threshold motor units (Burke et al. 1970). Similar observations have been reported in human motor units. Stimulation to the digital nerves of the index finger decreased the threshold of the high-threshold motor units and increased the threshold of the low-threshold motor units (Garnett and Stephens 1981). These threshold changes are equivalent to excitatory effects on the late-recruited,

⁵ For more information on motor units, see Appendix A: Motor Units

high-threshold motor units with contrasting inhibitory effects on the early-recruited, low-threshold motor units. Indeed, differential vestibular input to motor units has been observed in cats. Electrical stimulation to Deiter's nucleus projects to the lumbosacral region of the spinal cord (Wilson and Peterson 1981) and affects triceps surae motor units. The vestibulospinal volley created by stimulation to the vestibular nucleus is not uniformly distributed amongst the triceps surae motoneuron pool. Fast fatigable (type FF) motor neurons received 2.6x greater input than slow (type S) motor neurons (Westcott et al. 1995). To the best of our knowledge, similar interactions between descending vestibular pathways and lower limb motor units have not been investigated in humans. We believe based on research evidence documenting cutaneous afferent interactions with motor units in cats and humans and the above discussed vestibulospinal interactions with motor units in cats, that vestibular input has differential influence on soleus motor units in humans with a similar bias toward higher threshold motor units.

The purpose of this study was to investigate the contributions of the vestibular system using galvanic vestibular stimulation in quietly standing human subjects. Specifically, the goal of this research project was to determine the influence of descending vestibular input on individual motor units in the soleus muscle. We hypothesized that there would be non-uniform interactions between soleus motor units and GVS, such that the descending vestibular volley generated from GVS would have a greater influence on higher threshold motor units. Muscle responses from the right soleus were recorded from surface EMG placed on the medial and lateral portions of the muscle and intramuscular EMG inserted in the medial and lateral portions of the muscle at various depths. Multiple locations and depths of the surface and intramuscular EMG were

chosen to provide a good representation of the muscle. Global muscle responses were analyzed by trigger-averaging the rectified surface EMGs to the onset of the GVS pulse. To analyze vestibular influences on individual motor units, post-stimulus time histograms (PSTHs) were created to determine if there were modulations in motor unit firing rate. PSTHs were correlated to the global muscle responses to determine the contributions of the individual motor unit to the global GVS-evoked muscle response. Motor unit triggered-averages (MUTAs) were created to classify motor units into distinctive groups based on recruitment threshold. The results supported the hypothesis that there is a non-uniform influence from GVS-evoked vestibular input on soleus motor units. Specifically, vestibular input had a greater influence on motor units with larger MUTAs, and thus putative higher threshold motor units.

Materials and Methods

Participants

Fifteen university students (12 males and 3 females, aged 23-30) with no history of balance disorders, vestibular disorders, hearing deficits, lower limb injuries, or prior neuromuscular injuries (regardless of source) participated in this experiment. Participants provided written, informed consent prior to their participation. The procedures conformed to the standards of the Declaration of Helsinki and were approved by the University of British Columbia's clinical research ethics board.

Electromyography

Surface and intramuscular wire EMG were recorded from the right soleus muscle. For each subject, the right lower limb was shaved and cleaned with alcohol at the sites of electrode placement. The locations of the surface and intramuscular electrodes were chosen to record a good representation of the muscle and were as follows (Figure 1):

Surface Electrodes: Self-adhesive Ag/AgCl surface electrodes (Soft-E™ H59P: Kendall-LTP, Chicopee, MA, USA) were placed on the skin along the length of the right soleus muscle with an inter-electrode distance of 12 mm.

Lateral - Inferior to the gastrocnemius and lateral to the Achilles tendon.

Medial - Inferior to the gastrocnemius and medial to the Achilles tendon.

Intramuscular Wire Electrodes⁶: Stainless steel, hand-made intramuscular wire electrodes (Stainless Steel 304 H-ML, California Fine Wire Company, Grover Beach, USA) were inserted at the three specific locations in the right soleus muscle. The wires were inserted at various depths to capture a larger motor unit pool.

Wire 1 - Inferior to the gastrocnemius, lateral to the Achilles tendon, superficial insertion into the soleus muscle (1.0-1.5 cm depth) between lateral surface electrodes.

Wire 2 - Inferior to the gastrocnemius, lateral to the Achilles tendon, slightly medial to wire 1, deep insertion into the soleus muscle (2.0-2.5 cm depth) between lateral surface electrodes.

Wire 3 - Inferior to the gastrocnemius, medial to the Achilles tendon, superficial insertion into the soleus muscle (1.0-1.5 cm depth) between medial surface electrodes.

⁶ For more information on intramuscular EMG, see Appendix A: Intramuscular Wire Electrodes

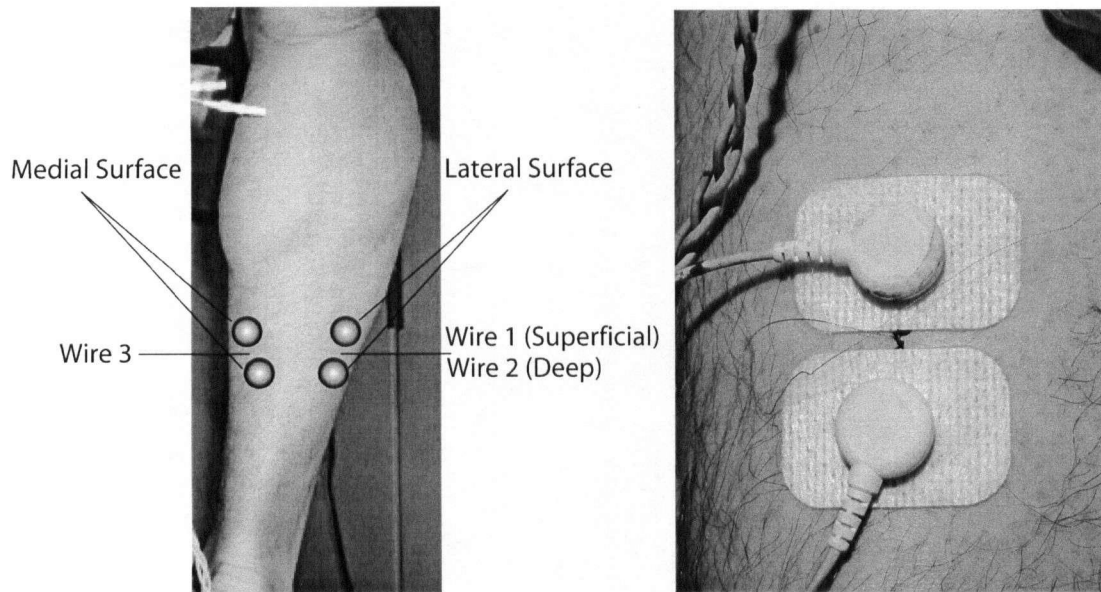


Figure 1. The sites of surface EMG placements and intramuscular wire EMG insertions. The figure on the left presents theoretical EMG positions on the posterior surface of the right soleus muscle. The figure on the right is an image of surface and intramuscular electrodes from an actual experimental setup of the right soleus.

Surface EMGs were amplified at 20k and bandpass filtered from 30 Hz to 1000 Hz (Grass P511, Grass Technologies, West Warwick, USA). Wire EMG signals were amplified at 2-5k and bandpass filtered from 300 Hz to 3000 Hz (Grass Model HZP and Grass P511, Grass Technologies, West Warwick, USA). EMG signals were digitized (6250 and 12500 Hz for surface and intramuscular signals respectively) through an A/D converter (Micro 1401, Cambridge Electronic Design, Cambridge UK).

Galvanic Vestibular Stimulation

GVS was delivered using a bipolar, binaural configuration. Two carbon-rubber stimulating electrodes (9 cm²) were placed behind the participant's ears, over the mastoid processes, and secured with an elastic headband. Output signals were sent from a

computer through a Micro 1401 interface (Cambridge Electronics Design, Cambridge, UK) which delivered a square-wave pulse through a constant-current analog stimulus isolation unit (Model 2200 Analog Stimulus Isolator: AM Systems, Carlsborg, WA). Short duration (30 ms), 4 mA GVS pulses were randomly delivered with an inter-stimulus interval ranging from 300-556 msec.

Experimental Task and Design

Each participant attended a single experimental session lasting approximately three hours. Subjects were instructed to stand quietly with their heads facing forward and eyes open. During each trial, the subjects were asked to keep their arms at their sides and to minimize extraneous body movements. Subjects stood on a force plate (Bertec 4060-80: Bertec Corp., Columbus, OH) with their feet 1-2 cm apart (measured at the medial malleoli) and their footprints were traced on paper. For each successive experimental trial, subjects placed their feet in the traced outlines to ensure consistent foot placement between trials. The session began with surface electrode placements and intramuscular electrode insertions while the subject was in a seated position. On occasion, more than three intramuscular insertion attempts were required to ensure easily identifiable motor units. No more than two attempts at each insertion site were required to record suitable motor units. Subjects performed six standing GVS trials and were exposed to 900 randomized GVS perturbations per trial (450 **anode right** configuration: anode right mastoid / cathode left mastoid; 450 **cathode right** configuration: cathode right mastoid / anode left mastoid (Figure 2)). Each subject received 5400 GVS pulses (2700 pulses for each GVS configuration) over the experiment.

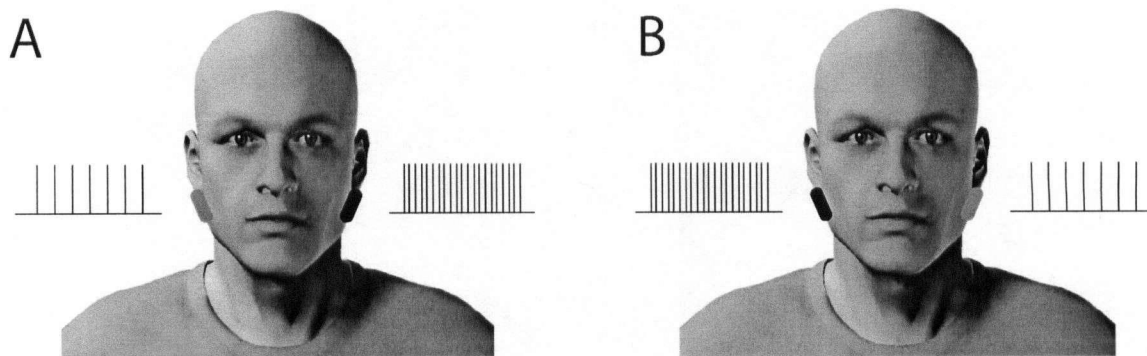


Figure 2. GVS electrode configurations, A: GVS **anode right** configuration (anode right mastoid / cathode left mastoid), B: GVS **cathode right** configuration (cathode right mastoid / anode left mastoid). The firing rates of the affected vestibular afferents are decreased on the side of the anode and are increased on the side of the cathode.

Data Analyses and Statistics

Surface EMG signals were full-wave rectified and trigger-averaged to the onset of the GVS pulse (Spike2 v5.13 software, Cambridge Electronic Design, Cambridge UK). Separate averages were performed for the anode right and cathode right GVS configurations. The EMG averages were analyzed from 50 msec prior to and 300 msec post GVS pulse. The onset latencies, peak-to-peak amplitudes, and peak latencies of the EMG responses were quantified using Matlab 7.0 (Mathworks Inc., Natick, MA). Onset latencies were determined using a log-likelihood-ratio algorithm (Stauder and Wolf 1999; Stauder 2001) and confirmed visually. Peak-to-peak amplitudes were determined as the amplitude differences between the maximum and minimum muscle responses observed between 50 and 300 msec after the GVS pulse. Peak latencies were determined as the time intervals between the onset of GVS and the time to maximum and minimum muscle response.

Individual motor units were identified from the digitized intramuscular EMG signal using a template-matching algorithm in Spike2 software⁷. To determine the firing probability of each motor unit with respect to the GVS pulse, PSTHs were constructed. For each motor unit, the occurrence of firing was binned in one of 175 individual bins from 50 msec prior to and 300 msec post GVS pulse (each bin was two msec in duration). The pre-stimulus mean and standard deviation firing probabilities were computed for each PSTH using the 25 bins prior to the GVS pulse (-50 to 0 msec prior to the pulse). Peaks and troughs in the PSTHs were considered significant when two consecutive bins differed from the pre-stimulus mean by more than two standard deviations or if one bin differed from the pre-stimulus mean by more than four standard deviations (Inglis et al. 1997). A PSTH significance score was created to quantify the response of the motor unit to the GVS stimuli. For every occurrence considered significantly different from the pre-stimulus mean that occurred between 50 – 150 msec after the GVS perturbation, a single point was added to the PSTH significance score. The scores from the anode right and cathode right GVS configurations were combined to provide a single score for each motor unit. A PSTH significance score equal to zero would signify that the motor unit was not affected by GVS, whereas a score greater than zero would signify that the motor unit was affected by GVS.

Linear correlations were calculated from the PSTH constructed for each motor unit and the surface EMG recorded from the electrodes superficial to the corresponding motor unit. The coefficient of correlation would describe if the variability of the individual motor unit's firing rate was modulated with surface EMG. Surface EMG averages were down-sampled to 500 Hz to match the equivalent number of histograms in

⁷ For more information on template-matching, see Appendix A: Template-Matching

the PSTHs. Coefficients of correlation (r) were calculated for each motor unit and each motor unit was categorized into one of two groups: R-Low (r value < 0.4) or R-High (r value > 0.4).

Individual motor units were classified based on unit triggered-averages of the surface EMG termed MUTAs. Raw, unrectified, surface EMG was trigger-averaged independently from the onset of each motor unit firing. MUTAs were measured from 20 msec prior to and 30 msec post individual motor unit firing. MUTAs were measured from the surface EMG ipsilateral to the wire EMG where the motor unit was recorded. Each MUTA was quantified by determining the peak-to-peak amplitude. Peak-to-peak amplitudes were normalized to the MUTA with the smallest peak-to-peak value within subjects and within the same surface EMG.

Two-tailed t -tests were performed using Statistica 6.0 software (Statsoft Inc., Tulsa, OK) to assess if onset latencies, peak-to-peak amplitudes, and peak latencies from the GVS-evoked muscle responses differed between GVS anode right and GVS cathode right conditions and between lateral and medial surface EMG recordings. Additionally Mann-Whitney U tests were performed to determine if the variables describing the R-High motor units were significantly greater than variables describing the R-Low motor units. Separate Mann-Whitney U tests were performed on PSTH significance scores and normalized MUTA peak-to-peak amplitudes between the R-Low and R-High motor unit groups with $\alpha \leq 0.05$.

Results

The data recorded from eleven of the fifteen participants were used in the analyses (Table 1). The four subjects who were not used in analysis did not produce easily identifiable motor units on any of the three intramuscular wire electrodes. All the results refer to the data collected only from those eleven subjects.

<i>Subject</i>	<i>Wire Electrode 1 (Lateral / Superficial)</i>	<i>Wire Electrode 2 (Lateral / Deep)</i>	<i>Wire Electrode 3 (Medial / Superficial)</i>
1	0	0	0
2	1	1	0
3	4	1	0
4	0	0	7
5	1	0	1
6	0	0	0
7	0	0	4
8	0	0	0
9	2	2	4
10	0	1	4
11	5	1	2
12	2	3	2
13	3	0	2
14	0	2	0
15	0	0	0
Total	18	11	26

Table 1. Number of motor units identified from each wire electrode for each subject. Fifty-five motor units were collected from all subjects.

GVS-Evoked Muscle Responses

Short duration GVS perturbations did not produce observable surface EMG responses from an individual stimulus (Figure 3). When trigger-averaged, consistent multiphasic EMG responses from the medial and lateral sections of the right soleus muscle were observed in all subjects and when averaged across all subjects (Figure 4). For each surface electrode, response onset latencies (Table 2), peak-to-peak amplitudes (Table 3), and peak latencies (Table 4) of the GVS-evoked muscle responses between anode right and cathode right GVS configurations were not statistically significant ($p > 0.05$). Additionally, response onset latencies (Table 2), peak-to-peak amplitudes (Table 3), and peak latencies (Table 4) of the GVS-evoked muscle responses between the lateral and medial surface electrodes were not statistically significant ($p > 0.05$). All onset latencies, peak-to-peak amplitudes, and peak latencies from both GVS conditions (anode right and cathode right) and surface EMG recordings (lateral and medial) were combined. The anode right configuration produced an initial increase in EMG activity (decrease for the cathode right configuration) with a mean onset latency of 58.3 (3.1) msec. A secondary EMG response with opposite polarities (GVS configuration dependent) occurred with a mean secondary onset latency of 98.5 (3.8) msec. The mean peak-to-peak amplitude of the GVS-evoked muscle response was 5.21 (2.95) μV . The mean peak latencies of GVS-evoked muscle responses was 82.2 (6.0) msec for the first peak and 130.1 (13.6) msec for the second peak.

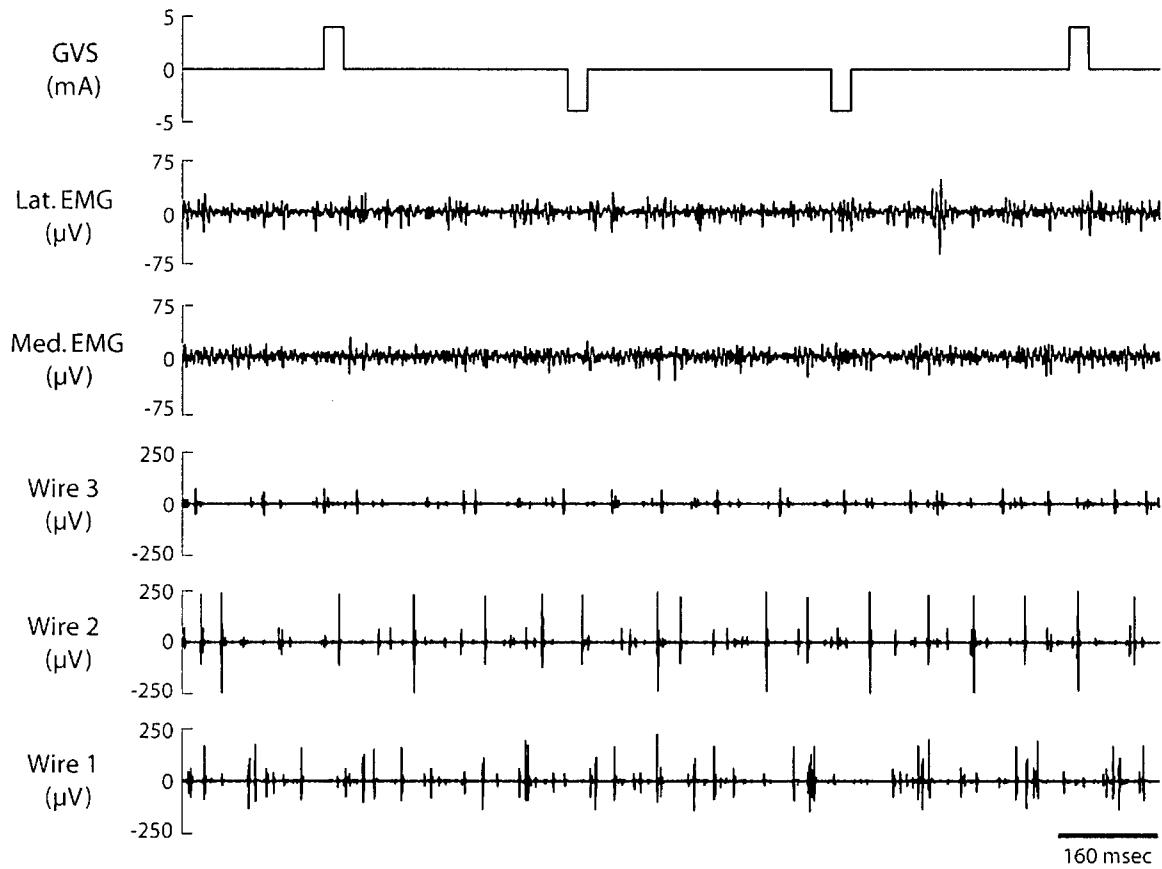


Figure 3. Raw data recorded from galvanic vestibular stimulation (GVS), surface electromyography (EMG) recorded from the lateral soleus (Lat.EMG), medial soleus (Med.EMG), and intramuscular EMG from wires 1 (lateral / superficial), 2 (lateral / deep), and 3 (medial / superficial). Identifiable muscle responses to GVS were not present in the surface and intramuscular EMG following a single perturbation of GVS.

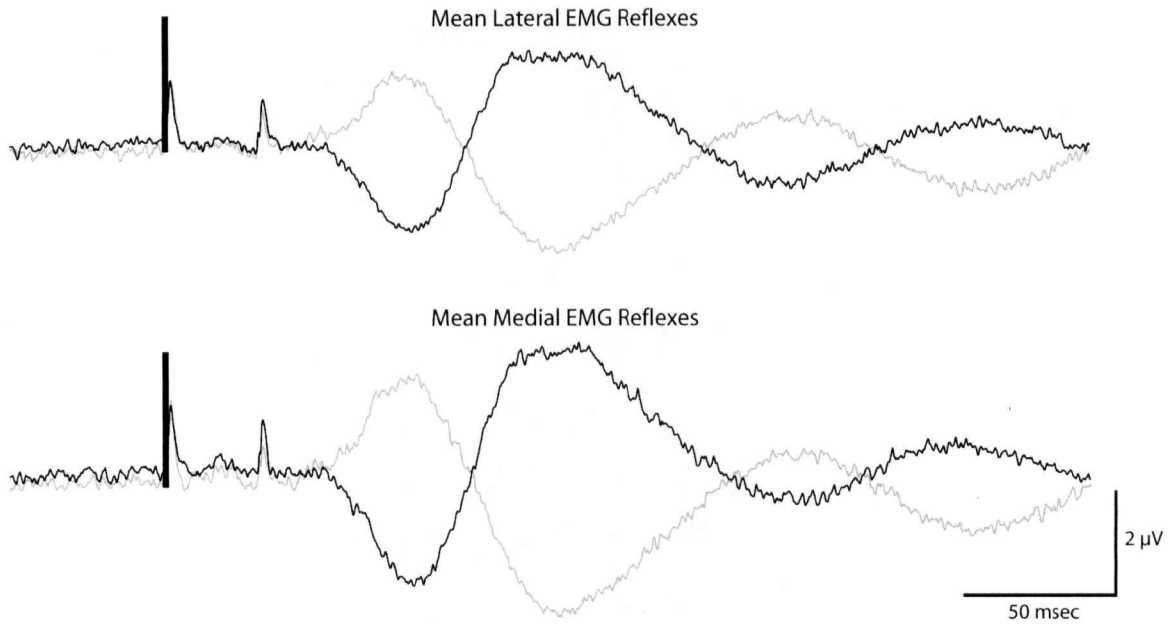


Figure 4. GVS-evoked muscle responses trigger-averaged from lateral and medial surface EMG recorded from the right soleus muscle averaged from all subjects ($n=11$). The bolded bar represents the onsets of the GVS perturbations. The grey muscle responses are from the GVS anode right configuration and the black muscle responses are from the GVS cathode right configuration. Note a sharp increase in EMG activity occurring at 30 msec after the GVS perturbation. The increase represents the offset of the GVS perturbation when the polarity of the current is reversed to return the current to zero mA.

<i>Subject</i>	<i>GVS Condition</i>	<i>Lateral EMG 1st response (msec)</i>	<i>Lateral EMG 2nd response (msec)</i>	<i>Medial EMG 1st response (msec)</i>	<i>Medial EMG 2nd response (msec)</i>
1	Anode	56.9	91.3	62.0	100.6
	Cathode	61.7	93.2	62.5	101.0
2	Anode	57.8	94.8	56.2	96.7
	Cathode	59.1	93.5	59.6	94.6
3	Anode	55.9	99.0	59.1	101.2
	Cathode	58.3	95.9	60.1	101.7
4	Anode	58.0	95.3	61.7	102.5
	Cathode	65.4	98.5	62.0	106.6
5	Anode	56.2	94.0	53.0	92.7
	Cathode	56.1	97.0	57.0	96.9
6	Anode	61.5	99.0	60.4	97.4
	Cathode	58.6	99.9	54.6	94.0
7	Anode	54.6	101.4	59.9	106.3
	Cathode	59.9	106.5	62.0	107.1
8	Anode	54.3	95.3	54.3	99.4
	Cathode	54.5	98.6	58.0	99.6
9	Anode	55.0	101.7	63.0	98.8
	Cathode	56.2	97.8	54.0	99.4
10	Anode	53.8	93.7	57.7	98.6
	Cathode	58.2	99.6	59.4	95.8
11	Anode	54.3	98.8	63.8	99.6
	Cathode	59.6	99.0	60.6	101.2
Mean		57.5 (2.9)	97.4 (3.5)	59.1 (3.1)	99.6 (3.9)

Table 2. Response onset latencies from the GVS-evoked soleus responses recorded from the lateral and medial surface EMGs. Anode represents the anode right GVS configuration and cathode represents the cathode right GVS configuration. Onset latencies from the anode right and cathode right configurations were combined independently for each surface EMG to determine mean values. The results from each subject are determined from the trigger-averaged EMG. The values in bold are means (SD).

<i>Subject</i>	<i>GVS Condition</i>	<i>Lateral EMG peak-to-peak (μV)</i>	<i>Medial EMG peak-to-peak (μV)</i>
1	Anode	1.70	6.05
	Cathode	1.54	5.99
2	Anode	7.74	11.15
	Cathode	7.42	10.54
3	Anode	6.35	11.45
	Cathode	5.76	11.11
4	Anode	3.02	2.57
	Cathode	3.66	2.79
5	Anode	9.84	10.30
	Cathode	9.07	7.92
6	Anode	3.60	3.69
	Cathode	3.68	3.60
7	Anode	5.50	5.25
	Cathode	5.84	5.74
8	Anode	3.09	1.11
	Cathode	3.56	1.14
9	Anode	2.07	2.38
	Cathode	2.47	2.72
10	Anode	3.10	4.84
	Cathode	3.56	4.77
11	Anode	2.86	6.76
	Cathode	4.05	8.04
Mean		4.53 (2.35)	5.91 (3.36)

Table 3. Peak-to-peak amplitudes from the GVS-evoked soleus responses recorded from the lateral and medial surface EMGs. Anode represents the anode right GVS configuration and cathode represents the cathode right GVS configuration. Peak-to-peak amplitudes from the anode right and cathode right configurations were combined independently for each surface EMG to determine mean values. The results from each subject are determined from the trigger-averaged EMG. The values in bold are means (SD).

<i>Subject</i>	<i>GVS Condition</i>	<i>Lateral EMG 1st peak latency (msec)</i>	<i>Lateral EMG 2nd peak latency (msec)</i>	<i>Medial EMG 1st peak latency (msec)</i>	<i>Medial EMG 2nd peak latency (msec)</i>
1	Anode	82.8	123.3	90.3	136.7
	Cathode	85.0	113.5	83.9	130.8
2	Anode	75.9	118.8	76.7	126.2
	Cathode	80.2	108.2	80.7	115.9
3	Anode	77.4	133.5	82.0	129.7
	Cathode	83.9	133.7	84.1	138.8
4	Anode	89.2	156.2	94.2	162.6
	Cathode	86.0	153.0	89.8	148.2
5	Anode	69.8	117.5	68.7	120.4
	Cathode	74.2	113.5	72.7	113.0
6	Anode	87.0	131.0	77.8	132.9
	Cathode	84.9	119.4	75.4	125.0
7	Anode	94.6	137.8	87.9	146.6
	Cathode	90.5	139.4	75.6	141.7
8	Anode	79.8	117.5	85.0	134.3
	Cathode	79.9	116.2	84.6	120.6
9	Anode	92.6	143.0	83.3	151.3
	Cathode	82.5	146.2	82.5	140.1
10	Anode	80.1	123.3	76.4	130.5
	Cathode	83.0	110.0	83.1	112.9
11	Anode	76.1	128.4	79.3	135.9
	Cathode	82.0	112.9	85.0	132.2
Mean		82.1 (6.1)	127.1 (14.1)	81.8 (6.1)	133.0 (12.6)

Table 4. Peak latencies from the GVS-evoked soleus responses recorded from lateral and medial surface EMG. Anode represents the anode right GVS configuration and cathode represents the cathode right GVS configuration. Peak latencies from the anode right and cathode right configurations were combined independently for each surface EMG to determine mean values. The results from each subject are determined from the trigger-averaged EMG. The values in bold are means (SD).

Motor Units

Individual motor units were identified and template-matched from the intramuscular wire electrodes (Figure 5). Fifty-five motor units were collected and analyzed. GVS-evoked responses recorded from individual motor units in the soleus muscle were not uniform. For example, the PSTHs constructed for certain motor units had distinct peaks and troughs significantly different from the pre-stimulation mean with onset latencies between 50-70 msec and 110-130 msec respectively (Figure 6). When present, the responses observed in the single motor unit PSTH were broad and relatively weak, but nevertheless corresponded to the polarity observed in the surface recordings. In contrast, the PSTHs constructed for other motor units did not possess distinct peaks and troughs different from the pre-stimulation mean (Figure 7). These motor units fired randomly with respect to the stimuli and were not affected by the GVS. Fourteen motor units were not influenced by GVS (PSTH significance score = 0) and the remaining forty-one motor units were influenced by GVS (PSTH significance score > 0). The instantaneous firing frequencies of the motor units were between 8-15 Hz. Throughout the entire experiment, the bandwidth of 8-15 Hz did not increase or decrease, but the instantaneous firing frequency varied within the bandwidth for each trial. PSTH significance scores ranged from a minimum of zero to a maximum of nineteen (Tables 5 and 6) with a mean score for all fifty-five motor units equal to 3.67 (4.76).

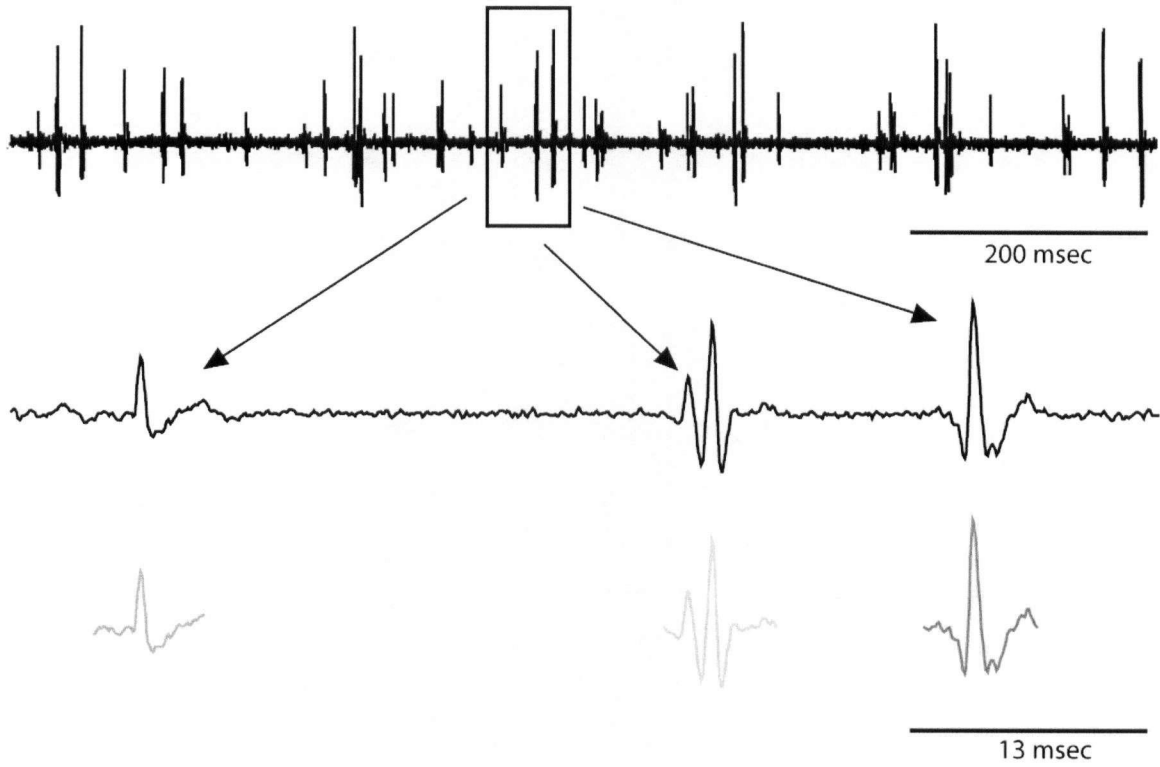


Figure 5. Raw, intramuscular EMG collected from a single subject and identification of three individual, unique motor units from a single wire electrode. Only distinct motor units that could be easily identified were used in analysis.

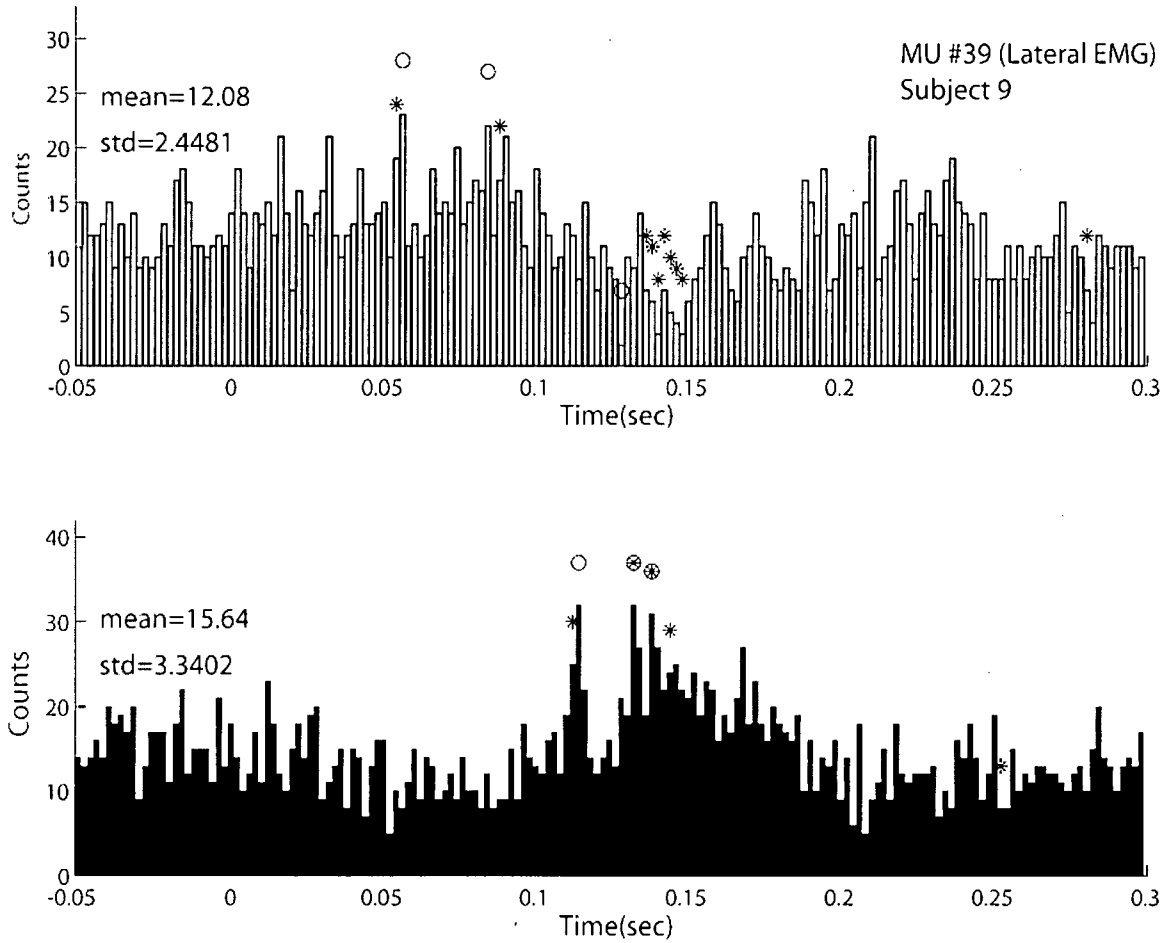


Figure 6. PSTH from a motor unit recorded from subject nine on wire two. The top PSTH is from the anode right GVS configuration and the bottom PSTH is from the cathode right GVS configuration. The onset of the GVS perturbation is at time zero. The pre-stimulus mean and standard deviation are presented for each PSTH. Asterisks represent two consecutive bins that are two standard deviations away from the pre-stimulus mean. Circles represent one bin that is four standard deviations away from the pre-stimulus mean. The PSTH significance score for this individual motor unit is nineteen.

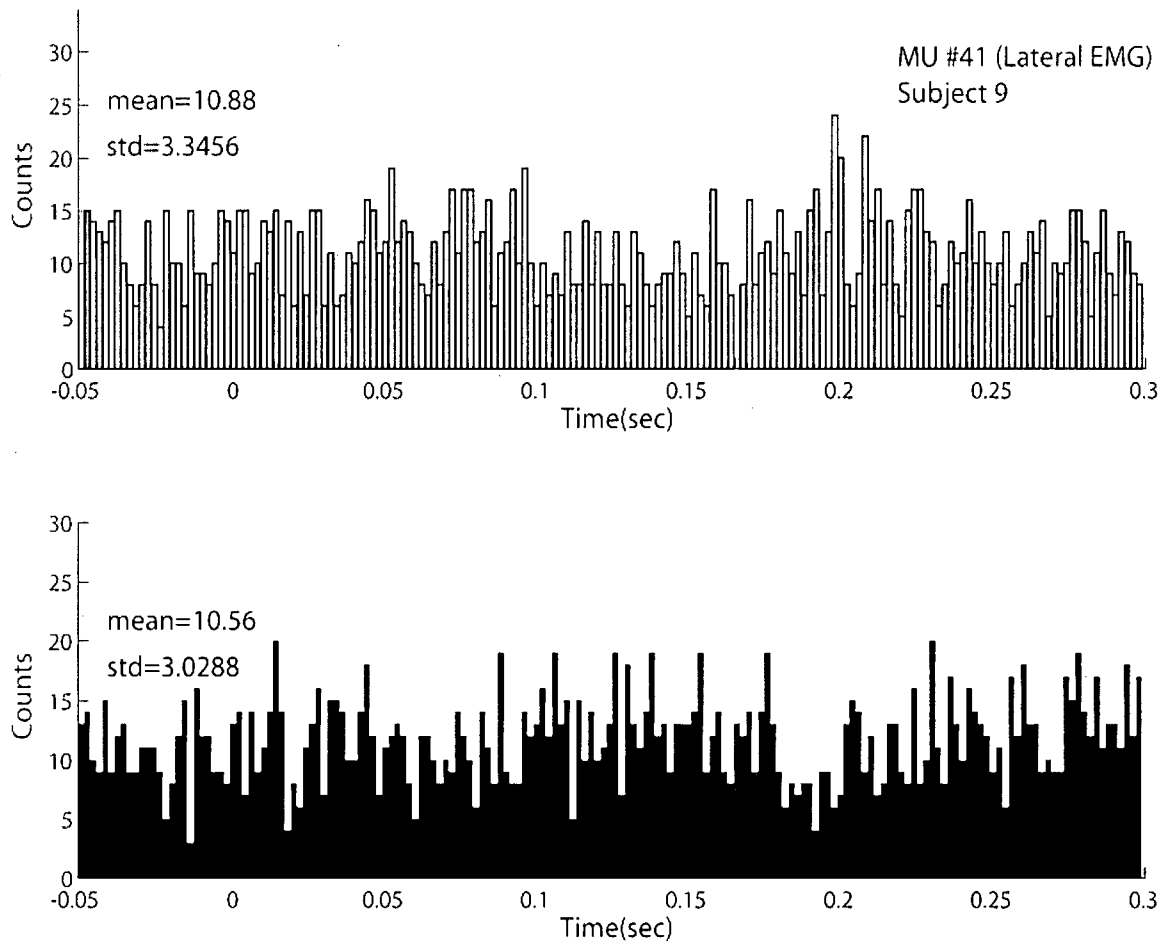


Figure 7. PSTH from a motor unit that is recorded from the same subject (nine) and same wire (two) as the motor unit analyzed in figure 7. The top PSTH is from the anode right GVS configuration and the bottom PSTH is from the cathode right GVS configuration. The onset of the GVS perturbation is at time zero. The pre-stimulus mean and standard deviation are presented for each PSTH. The PSTH significance score for this individual motor unit is zero.

<i>r Value</i>	<i>PSTH Significance Score</i>	<i>MUTA peak-to-peak amplitude (mV)</i>	<i>Normalized MUTA peak-to-peak amplitude (ratio)</i>
-0.217	3	0.011	N/A
-0.122	2	0.002	1.215
0.008	0	0.067	10.578
0.064	0	0.006	1.000
0.111	0	0.016	1.000
0.126	0	0.004	1.000
0.136	0	0.010	N/A
0.162	0	0.002	1.000
0.165	0	0.004	1.000
0.182	0	0.019	1.221
0.184	1	0.053	N/A
0.197	0	0.009	4.369
0.208	2	0.031	6.538
0.264	4	0.035	5.497
0.264	0	0.073	8.275
0.285	4	0.005	1.000
0.295	1	0.013	N/A
0.324	1	0.049	1.000
0.352	2	0.009	1.000
0.364	0	0.005	1.128
0.372	1	0.008	N/A

Table 5. Individual motor units that were categorized into the R-Low group ($r < 0.4$). Note that some motor units did not have a complementary R-High ($r > 0.4$) motor unit and therefore their normalized MUTA peak-to-peak amplitudes were not calculated.

<i>r Value</i>	<i>PSTH Significance Score</i>	<i>MUTA peak-to-peak amplitude (mV)</i>	<i>Normalized MUTA peak-to-peak amplitude (ratio)</i>
0.409	1	0.016	3.502
0.414	6	0.002	N/A
0.430	2	0.046	7.376
0.457	3	0.100	11.331
0.463	1	0.011	N/A
0.482	2	0.030	0.605
0.486	5	0.013	6.880
0.525	11	0.003	N/A
0.528	4	0.017	N/A
0.539	2	0.017	0.349
0.553	3	0.009	0.558
0.559	0	0.007	1.567
0.567	2	0.017	N/A
0.571	13	0.020	4.151
0.595	2	0.012	N/A
0.600	14	0.029	N/A
0.600	1	0.034	N/A
0.611	0	0.009	N/A
0.615	0	0.006	N/A
0.616	5	0.023	N/A
0.618	2	0.090	10.165
0.621	11	0.002	1.131
0.642	3	0.006	N/A
0.646	2	0.007	0.833
0.652	4	0.002	1.235
0.664	4	0.029	N/A
0.666	7	0.034	N/A
0.675	4	0.036	2.254
0.677	2	0.034	9.609
0.686	19	0.040	8.391
0.713	12	0.028	N/A
0.727	2	0.007	3.840
0.741	19	0.029	6.455
0.812	13	0.015	7.483

Table 6. Individual motor units that were categorized into the R-High group ($r > 0.4$). Note that some motor units did not have a complementary R-Low ($r < 0.4$) motor unit and therefore their normalized MUTA peak-to-peak amplitudes were not calculated.

Motor Unit Classification

Correlations between GVS-evoked muscle responses and PSTHs were not uniform amongst all motor units. Twenty-one motor units were classified into the R-Low group and the remaining thirty-four motor units were classified into the R-High group. Motor units that were categorized into the R-Low group had r values that ranged from -0.217 to 0.372 (Table 5) and motor units that were categorized into the R-High group had r values that ranged from 0.409 to 0.812 (Table 6).

PSTH significance scores calculated for motor units categorized into R-Low and R-High groups (Figure 8) ranged from zero to four for the R-Low group (Table 5) and zero to 19 for the R-High group (Table 6). There was a significant effect for PSTH significance scores, $U = 122.5$, $p < 0.05$, with the mean PSTH significance score of the R-High motor units of 5.324 (5.347) being greater than the R-Low PSTH significance score of 1.000 (1.342) (Figure 9).

Normalized MUTA peak-to-peak amplitudes were calculated only for motor units that possessed a complementary motor unit from the same intramuscular wire, but in the contrasting R-group. Normalized peak-to-peak amplitudes from the R-Low MUTAs ($n = 16$) ranged from one to ten times the amplitude of the smallest R-Low MUTA (Table 5). The normalized peak-to-peak amplitudes from the R-High MUTAs ($n = 19$) ranged from half to eleven times the amplitude of the smallest R-Low MUTA (Table 6). There was no significant effect for peak-to-peak amplitudes determined from normalized MUTAs, $U = 113.0$, $p = 0.097$, with the mean peak-to-peak amplitude of the R-High group being 1.6 times greater than the mean peak-to-peak amplitude of the R-Low group (Figure 9).

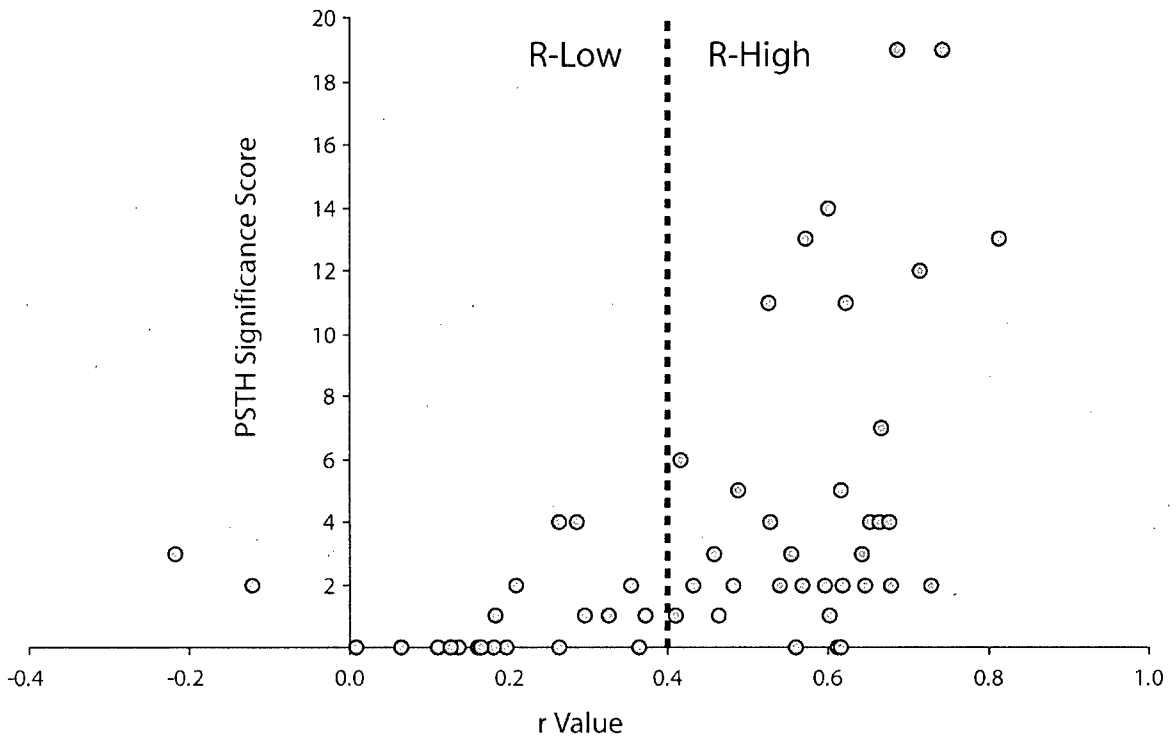


Figure 8. Fifty-five motor unit PSTHs were correlated to their respective surface EMG response. The r value was plotted against the PSTH significance score. The two groups: R-Low ($r < 0.04$) and R-High ($r > 0.04$) are separated by the dotted line.

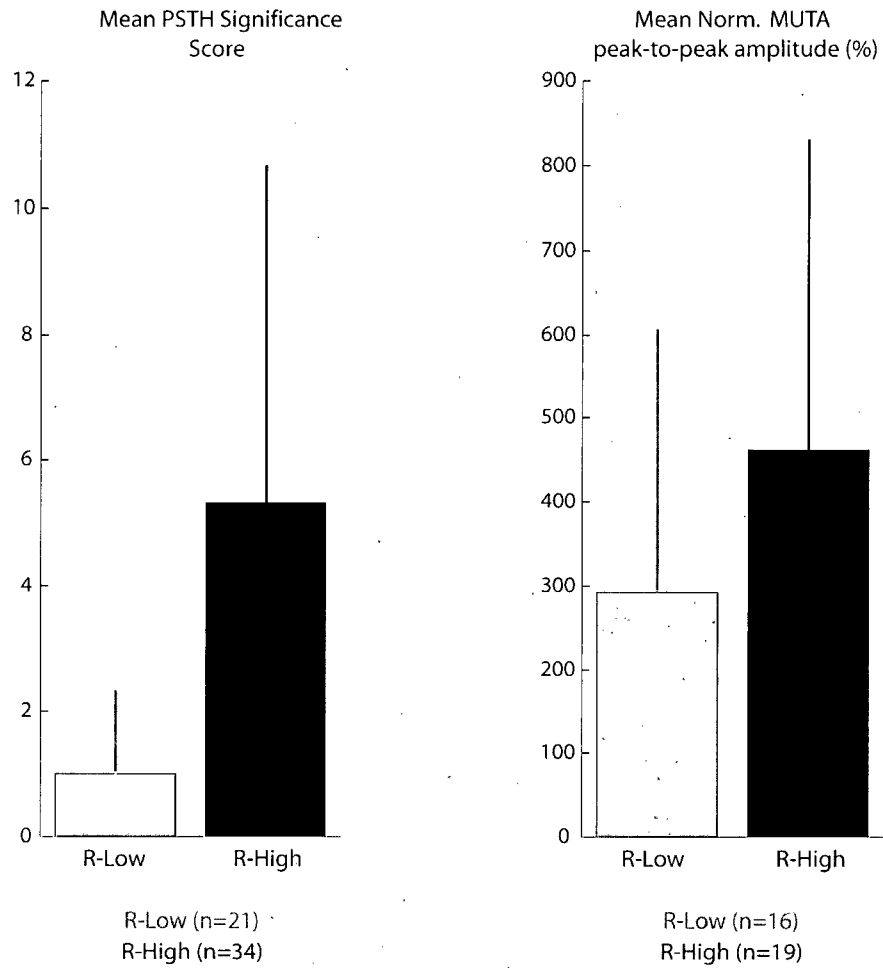


Figure 9. Mean PSTH significance scores and normalized MUTA peak-to-peak amplitudes for R-Low and R-High motor units. The bars represent one standard deviation away from the mean. Note the number of motor units used in each analysis: fewer motor units were used in the normalized MUTA peak-to-peak analyses due to no complementary motor units in the contrasting R group for certain wire electrodes.

Discussion

Short duration galvanic vestibular stimuli applied to subjects standing upright with their heads facing forward evoked stereotyped muscular responses in the right soleus recorded from surface electrodes. GVS-evoked muscle responses analyzed from the surface EMG were multiphasic and possessed the same polarities from both the lateral and medial surfaces of the muscle (GVS configuration dependant). In contrast, the GVS-evoked muscle responses analyzed from the intramuscular EMG were not uniform across all motor units recorded from the soleus muscle. PSTH significance scores ranged from zero to nineteen suggesting differential motor unit responses to GVS perturbations. Additionally, PSTH significance scores lay upon a spectrum rather than a dual response (the motor unit being affected by GVS or the motor unit not being affected by GVS). The range to which GVS affects motor units suggests that the gain of the descending vestibular-evoked volley is not uniform for all motor units in soleus. R values correlating the PSTHs to the surface EMG responses also ranged from being not correlated to strongly correlated. The variable PSTH significance scores and r values support the hypothesis that vestibular projections modulated by GVS have a non-uniform influence on soleus motor units. Furthermore, motor unit classification suggests that vestibular influences modulated by GVS have a greater influence on relatively higher threshold motor units collected in this experiment. Although the results suggest preferential bias to higher threshold motor units, we cannot conclude that these motor units are indeed type FR or type FF because the determinant used to classify threshold in this study is a relative measure and not an absolute measure. Motor units with larger r values had MUTAs that were 1.6x larger than MUTAs from motor units with smaller r values. The results from

the present study support our hypothesis that there are non-uniform interactions between the vestibular system and the soleus motoneuron pool. Specifically, descending vestibular neural signals have a greater influence on relatively higher threshold motor units.

GVS-Evoked Muscle Responses

The observed biphasic responses in the right soleus muscle to short duration GVS stimuli have been reported previously with the subjects heads turned to the side (Britton et al. 1993; Watson and Colebatch 1998; Ali et al. 2003) and reported once with the subjects heads facing forward (Lee Son et al. 2005). The onset and peak latencies of the biphasic muscle responses in the present study are congruent with the latencies reported by previous authors. An initial facilitation or inhibition of muscle activity (GVS configuration dependent) was observed approximately 60 msec after the onset of the GVS perturbation. A secondary response of opposite polarity to the initial muscle response was observed approximately 95 msec after the onset of the GVS perturbation. GVS-evoked muscle responses analyzed from surface EMG provide a global estimate of the responses from individual motor units. The GVS-evoked muscle responses provide evidence that descending vestibular input affects the soleus motoneuron pool, but cannot characterize the contributions from individual motor units within the motoneuron pool.

Interactions between Vestibular and Somatosensory Inputs

Stimulation of cutaneous afferents in cats and humans and stimulation of vestibular nuclei in cats demonstrate non-uniform connections between afferent signals

from the present study present similar non-uniform connections between vestibular input and soleus motor units in quiet standing humans. For certain motor units, there were no significant modifications in firing probability of the single motor unit during the time frame of the GVS-evoked muscle response. In contrast, certain motor units increased or decreased their probability of firing by a factor of four during the time frame of the GVS-evoked muscle response. The motor units affected by the GVS pulses exhibited broad periods of excitation or inhibition in their PSTHs. This contrasts with the sharp, distinct peaks in the PSTHs observed for the monosynaptic projections to flexor carpi radialis motor units from median nerve stimulation (Inglis et al. 1997). The PSTH results from the present study could suggest oligosynaptic projections from the vestibular nuclei to the lower limb motor units (Inglis et al. 1997). Additionally, the descending vestibular projections are likely integrated with other spinal cord pathways. It is likely that activation of somatosensory afferents activated from the postural task interact with the descending neural signal generated from the brainstem.

One possible level of the interaction between vestibular and somatosensory afferents is at the spinal cord interneuron level (Kennedy et al. 2004). A likely candidate for somatosensory influence on descending vestibulospinal drive is presynaptic modulation of Ia projections to the motoneuron pool. This mechanism has been proposed to explain the alteration in activation onset and initial firing frequency of motor units elicited by GVS when the gastrocnemius muscle is shortened (Kennedy et al. 2004). Somatosensory integrations with descending vestibular projections are also observed in GVS standing paradigms. Limb loading through asymmetrical stance alters lateral ground reaction forces elicited by GVS perturbations (Marsden et al. 2002; Marsden et al. 2003).

Marsden et al. suggested that somatosensory skin, muscle, tendon, or joint receptors could contribute to the load-related changes in the GVS-evoked ground reaction forces. Iles and Pisini (1992) further mentioned changes in GVS-evoked muscle responses in soleus with a load-induced reduction. The results from the present study provide further evidence that the pathway between vestibular input on the spinal cord and the soleus motoneuron pool is not direct and is more than likely modulated by spinal cord reflexes generated by somatosensory receptors.

Continuum of Vestibular Connectivity to Soleus Motor Units

Spinal reflexes affect descending vestibulospinal projections to lower limb motoneuron pools (Iles and Pisini 1992; McCrea 1996). The results from the present study suggest that the degree to which the reflexes adjust the gain of the motor unit response is dependent on the motor unit's characteristics. MUTAs provide an indirect way of characterizing the threshold of individual motor units. Larger amplitude MUTAs are generated from greater amounts of recorded surface EMG. Assuming that Henneman's size principle and orderly recruitment are true, motor units that are recruited at the latter end of force production when surface EMG activity is great are higher threshold motor units. Hence, larger amplitude MUTAs could be representative of two options: a large proportion of slow-twitch muscle fibres contributing to the surface average or a small proportion of fast-twitch muscle fibres contributing to the surface average. Assuming that the second option is correct (Lemon et al. 1990; Jones et al. 1994), vestibular input has a greater influence on higher threshold motor units. The bias towards higher threshold, larger force producing motoneurons may increase the gain of

the input-output function of the motoneuron pool. Small increments in vestibular input will elicit large force changes from activation of high-threshold motoneurons. The compressed range of motor units activated by vestibular projections suggests that during quiet standing, the vestibular system may generate large force producing contractions in soleus to help control postural sway. In standing humans, Lee Son et al. (2005) showed an increase in gain of the GVS-evoked muscle response in soleus and tibialis anterior with increasing background muscle activity. We hypothesized that higher threshold motor units recruited during times of increased background muscle activity could be influenced largely by GVS to produce the observed results. MUTA analyses from the present study confirms the hypothesis that GVS has a greater effect on relatively higher threshold motor units collected in this study with respect to all the motor units collected.

Limitations

In the current study, motor unit classification was performed through indirect analysis. MUTAs follow the assumption that larger MUTAs represent the latter portion of the motor unit recruitment spectrum. Although this method is a suitable indirect procedure, a more precise mode of motor unit classification is necessary to confirm which motor units are affected by artificial vestibular disturbances. PSTH significance scores provide an index to which motor unit firing rates are modulated by GVS. The scores do not provide the relationships of the modulated motor unit firing rates to the GVS-evoked muscle responses, i.e. a high score would suggest many bins that are different from the mean, but does not necessarily suggest the shape of the PSTH is congruent to the muscle response. Classification of the motor units into R-Low and R-

High groups can imply incorrect interpretations of motor unit thresholds. It is likely that motor units are not categorized into slow, small force producing motor units versus fast, large force producing motor units, but rather classified based on a continuum. Intramuscular wire electrode technique requires precision to ensure the recording is collected from the correct muscle at the specified depth. The present study examined the lateral and medial portions of the soleus muscle inferior to the heads of the gastrocnemius muscle. Insertion at these locations into the soleus is not difficult. There are no superficial or deep muscles with respect to the soleus allowing insertion to be straightforward. In contrast, future studies using wire electrodes in less accessible muscles, such as the superior portions of soleus located deep to gastrocnemius, would require the use of ultrasound to provide the experimenter with precision during insertion.

Conclusions

The results from the present study have shown non-uniform motor unit responses in the soleus muscle to vestibular perturbations in humans standing upright with their heads facing forward. Differential connectivity between vestibular nuclei and lower limb motor units is likely generated from the integration of descending vestibular projections and spinal cord reflexes generated from peripheral afferent receptors. Galvanic pulses applied to vestibular afferents had a greater influence on higher threshold motor units than lower threshold motor units in the soleus muscle. Perhaps having the soleus motoneuron pool set up like this facilitates adequate levels of force production to counter naturally occurring body oscillations and help control postural sway. Based on the results found in the present study, future directions for GVS-quiet standing paradigms should

include further investigation into the relationships between descending vestibular input and spinal reflexes generated from the postural task or diagnostic possibilities to investigate the integrities of the descending pathways.

References

- Ali AS, Rowen KA, Iles JF (2003) Vestibular actions on back and lower limb muscles during postural tasks in man. *J Physiol* 546: 615-624
- Bacsi AM, Colebatch JG (2003) Anodal vestibular stimulation does not suppress vestibular reflexes in human subjects. *Exp Brain Res* 150: 525-528
- Bacsi AM, Colebatch JG (2005) Evidence for reflex and perceptual vestibular contributions to postural control. *Exp Brain Res* 160: 22-28
- Bacsi AM, Watson SR, Colebatch JG (2003) Galvanic and acoustic vestibular stimulation activate different populations of vestibular afferents. *Clin Neurophysiol* 114: 359-365
- Bent LR, Inglis JT, McFadyen BJ (2004a) When is vestibular information important during walking? *J Neurophysiol* 92: 1269-1275
- Bent LR, McFadyen BJ, Inglis JT (2004b) Is the use of vestibular information weighted differently across the initiation of walking? *Exp Brain Res* 157: 407-416
- Britton TC, Day BL, Brown P, Rothwell JC, Thompson PD, Marsden CD (1993) Postural Electromyographic Responses in the Arm and Leg Following Galvanic Vestibular Stimulation in Man. *Experimental Brain Research* 94: 143-151
- Burke RE (1981) Motor units: anatomy, physiology and functional organization. In: *Handbook of Physiology. The Nervous System. Motor Control*. Am. Physiol. Soc., Bethesda, MD
- Burke RE, Jankowska E, ten Bruggencate G (1970) A comparison of peripheral and rubrospinal synaptic input to slow and fast twitch motor units of triceps surae. *J Physiol* 207: 709-732
- Carlsen AN, Kennedy PM, Anderson KG, Cressman EK, Nagelkerke P, Chua R (2005) Identifying visual-vestibular contributions during target-directed locomotion. *Neurosci Lett* 384: 217-221
- Day BL, Fitzpatrick RC (2005) The vestibular system. *Curr Biol* 15: R583-586

- Dietz V (1992) Human neuronal control of automatic functional movements: interaction between central programs and afferent input. *Physiol Rev* 72: 33-69
- Edgerton VR, Smith JL, Simpson DR (1975) Muscle fibre type populations of human leg muscles. *Histochem J* 7: 259-266
- Enoka RM (2002) *Neuromechanics of human movement*. Human Kinetics, Champaign, Ill.
- Fernandez C, Goldberg JM (1971) Physiology of peripheral neurons innervating semicircular canals of the squirrel monkey. II. Response to sinusoidal stimulation and dynamics of peripheral vestibular system. *J Neurophysiol* 34: 661-675
- Fitzpatrick R, Burke D, Gandevia SC (1994) Task-dependent reflex responses and movement illusions evoked by galvanic vestibular stimulation in standing humans. *J Physiol* 478 (Pt 2): 363-372
- Fitzpatrick RC, Day BL (2004) Probing the human vestibular system with galvanic stimulation. *J Appl Physiol* 96: 2301-2316
- Fitzpatrick RC, Wardman DL, Taylor JL (1999) Effects of galvanic vestibular stimulation during human walking. *J Physiol* 517 (Pt 3): 931-939
- Garnett R, Stephens JA (1981) Changes in the recruitment threshold of motor units produced by cutaneous stimulation in man. *J Physiol* 311: 463-473
- Goldberg JM (2000) Afferent diversity and the organization of central vestibular pathways. *Exp Brain Res* 130: 277-297
- Goldberg JM, Smith CE, Fernandez C (1984) Relation between discharge regularity and responses to externally applied galvanic currents in vestibular nerve afferents of the squirrel monkey. *J Neurophysiol* 51: 1236-1256
- Goldberg ME, Hudspeth AJ (2000) The Vestibular System. In: Kandel ER, Schwartz JH, Jessell TM (eds) *Principles of Neural Science*. McGraw-Hill Health Professions Division, New York, pp 801-815

- Harris AJ, Duxson MJ, Butler JE, Hodges PW, Taylor JL, Gandevia SC (2005) Muscle fiber and motor unit behavior in the longest human skeletal muscle. *J Neurosci* 25: 8528-8533
- Henneman E, Mendell LM (1981) Functional organization of motoneuron pool and its inputs. In: *Handbook of Physiology. The Nervous System. Motor Control*. Am. Physiol. Soc., Bethesda, MD
- Iles JF, Pisini JV (1992) Vestibular-evoked postural reactions in man and modulation of transmission in spinal reflex pathways. *J Physiol* 455: 407-424
- Inglis JT, Meunier S, Leeper JB, Burke D, Gandevia SC (1997) Weak short-latency spinal projections to the long flexor of the human thumb. *Exp Brain Res* 115: 165-168
- Inglis JT, Shupert CL, Hlavacka F, Horak FB (1995) Effect of galvanic vestibular stimulation on human postural responses during support surface translations. *J Neurophysiol* 73: 896-901
- Jankelowitz SK, Colebatch JG (2004) Galvanic evoked vestibulospinal and vestibulocollic reflexes in stroke. *Clin Neurophysiol* 115: 1796-1801
- Jones KE, Lyons M, Bawa P, Lemon RN (1994) Recruitment order of motoneurons during functional tasks. *Exp Brain Res* 100: 503-508
- Kennedy PM, Carlsen AN, Inglis JT, Chow R, Franks IM, Chua R (2003) Relative contributions of visual and vestibular information on the trajectory of human gait. *Exp Brain Res* 153: 113-117
- Kennedy PM, Cresswell AG, Chua R, Inglis JT (2004) Galvanic vestibular stimulation alters the onset of motor unit discharge. *Muscle Nerve* 30: 188-194
- Kennedy PM, Inglis JT (2001) Modulation of the soleus H-reflex in prone human subjects using galvanic vestibular stimulation. *Clin Neurophysiol* 112: 2159-2163
- Kiernan JA, Barr ML (1998) Barr's The human nervous system : an anatomical viewpoint. Lippincott-Raven, Philadelphia

- Lee Son G, Blouin JS, Inglis JT (2005) Assessing the modulations in vestibulospinal sensitivity during quiet standing using galvanic vestibular stimulation. In: Neuroscience 2005, Washington, DC
- Lemon RN, Mantel GW, Rea PA (1990) Recording and identification of single motor units in the free-to-move primate hand. *Exp Brain Res* 81: 95-106
- Loeb GE, Ghez C (2000) The Motor Unit and Muscle Action. In: Kandel ER, Schwartz JH, Jessell TM (eds) *Principles of Neural Science*. McGraw-Hill Health Professions Division, New York, pp 674-694
- Lund S, Broberg C (1983) Effects of different head positions on postural sway in man induced by a reproducible vestibular error signal. *Acta Physiol Scand* 117: 307-309
- Marsden JF, Blakey G, Day BL (2003) Modulation of human vestibular-evoked postural responses by alterations in load. *J Physiol* 548: 949-953
- Marsden JF, Castellote J, Day BL (2002) Bipedal distribution of human vestibular-evoked postural responses during asymmetrical standing. *J Physiol* 542: 323-331
- McCrea DA (1996) Supraspinal and segmental interactions. *Can J Physiol Pharmacol* 74: 513-517
- Minor LB, Goldberg JM (1991) Vestibular-nerve inputs to the vestibulo-ocular reflex: a functional-ablation study in the squirrel monkey. *J Neurosci* 11: 1636-1648
- Nashner LM, Wolfson P (1974) Influence of head position and proprioceptive cues on short latency postural reflexes evoked by galvanic stimulation of the human labyrinth. *Brain Res* 67: 255-268
- Pastor MA, Day BL, Marsden CD (1993) Vestibular induced postural responses in Parkinson's disease. *Brain* 116 (Pt 5): 1177-1190
- Pavlik AE, Inglis JT, Lauk M, Oddsson L, Collins JJ (1999) The effects of stochastic galvanic vestibular stimulation on human postural sway. *Exp Brain Res* 124: 273-280

- Peterka RJ, Benolken MS (1995) Role of somatosensory and vestibular cues in attenuating visually induced human postural sway. *Exp Brain Res* 105: 101-110
- Pfaltz CR, Koike Y (1968) Galvanic test in central vestibular lesions. *Acta Otolaryngol* 65: 161-168
- Rosengren SM, Colebatch JG (2002) Differential effect of current rise time on short and medium latency vestibulospinal reflexes. *Clin Neurophysiol* 113: 1265-1272
- Rothwell JC (1994) Control of human voluntary movement. Chapman & Hall, London ; New York
- Séverac Cauquil A, Faldon M, Popov K, Day BL, Bronstein AM (2003) Short-latency eye movements evoked by near-threshold galvanic vestibular stimulation. *Exp Brain Res* 148: 414-418
- Speigal EA, Scala NP (1943) Response of the labyrinth apparatus to electrical stimulation. *Arch Otolaryngol* 38: 131-138
- Staude G, Wolf W (1999) Objective motor response onset detection in surface myoelectric signals. *Med Eng Phys* 21: 449-467
- Staude GH (2001) Precise onset detection of human motor responses using a whitening filter and the log-likelihood-ratio test. *IEEE Trans Biomed Eng* 48: 1292-1305
- Tokita T, Ito Y, Takagi K (1989) Modulation by head and trunk positions of the vestibulo-spinal reflexes evoked by galvanic stimulation of the labyrinth. Observations by labyrinthine evoked EMG. *Acta Otolaryngol* 107: 327-332
- Tortora GJ, Grabowski SR (2003) Principles of anatomy and physiology. Wiley, New York
- Watson SR, Colebatch JG (1997) EMG responses in the soleus muscles evoked by unipolar galvanic vestibular stimulation. *Electroencephalogr Clin Neurophysiol* 105: 476-483

- Watson SR, Colebatch JG (1998) Vestibular-evoked electromyographic responses in soleus: a comparison between click and galvanic stimulation. *Exp Brain Res* 119: 504-510
- Watson SR, Welgampola MS, Colebatch JG (2003) EMG responses evoked by the termination of galvanic (DC) vestibular stimulation: 'off-responses'. *Clin Neurophysiol* 114: 1456-1461
- Welgampola MS, Colebatch JG (2001) Vestibulospinal reflexes: quantitative effects of sensory feedback and postural task. *Exp Brain Res* 139: 345-353
- Welgampola MS, Colebatch JG (2002) Selective effects of ageing on vestibular-dependent lower limb responses following galvanic stimulation. *Clin Neurophysiol* 113: 528-534
- Westcott SL, Powers RK, Robinson FR, Binder MD (1995) Distribution of vestibulospinal synaptic input to cat triceps surae motoneurons. *Exp Brain Res* 107: 1-8
- Wilson VJ, Peterson BW (1981) Vestibulospinal and reticulospinal systems. In: *Handbook of Physiology. The Nervous System. Motor Control*. Am. Physiol. Soc., Bethesda, MD
- Wolf SL, Ammerman J, Jann B (1998) Organization of responses in human lateral gastrocnemius muscle to specified body perturbations. *J Electromyogr Kinesiol* 8: 11-21

APPENDIX A:
LITERATURE REVIEW

Vestibular System

For posture and gait, sensory inputs from visual, somatosensory, and vestibular afferents are integrated with central programs, such as the postural control system, to make adjustments to fulfill the requirements needed to complete the specified movement (Dietz 1992). Located in the inner ear, the vestibular apparatuses provide the brain with afferent information regarding accelerations of the head (Day and Fitzpatrick 2005). The vestibular system is comprised of two components that are tightly attached to the skull: semicircular canals and otolith organs. Together they code primarily for angular (semicircular canals) and linear (otolith organs) accelerations (Goldberg and Hudspeth 2000). Both components of the vestibular system contain mechanoreceptors that are stimulated through head accelerations. These mechanoreceptors are termed hair cells and are present in the vestibular apparatus with their cilia extruding into extracellular space. The cilia are classified into two types: stereocilia (multiple units per hair cell) or kinocilium (single unit per hair cell). Stimulation of the hair cells is initiated based on the positional relationship between the two types of cilia. For example, certain accelerations of the head will cause deflection of the stereocilia toward the kinocilium. These accelerations will increase the release of neurotransmitters, which will depolarize the hair cells and increase the discharge rate of the vestibular nerve. In contrast, other accelerations will cause deflection of the stereocilia away from the kinocilium. These accelerations will decrease the release of neurotransmitters, which will hyperpolarize the hair cells and decrease the discharge rate of the vestibular nerve.

The vestibular apparatuses are located on both sides of the head in the inner ear and are arranged as mirror opposites of each other. There are three semicircular canals

per apparatus (termed the horizontal, anterior, and posterior canals) which detect angular accelerations in three orthogonal axes. The three canals are situated along Reid's stereotactic line (bottom of inner orbital to auditory canal) and code for yaw (horizontal canal), roll (anterior and posterior canals), and pitch (anterior and posterior canals). Each canal is a closed tube filled with endolymph fluid. There is a large dilation in each canal called the ampulla. At this location, a gelatinous membrane termed the cupula extends across the canal and houses the cilia of the hair receptors. As angular accelerations of the head are made, the inertial forces of the fluid cause the hair cells to deflect in the opposite direction to the movement. Because all the hair cells in each canal share a common alignment, the neural signal that arises from angular accelerations of the head is identical throughout the entire canal.

There are two otolith organs per apparatus (termed the utricle and saccule) which detect linear accelerations. The otolith organs are orthogonal to each other with the utricle aligned backward from the horizontal by 30 degrees and sloping away laterally by 10 degrees and the saccule aligned in the sagittal plane (Fitzpatrick and Day 2004). The utricle codes primarily for lateral accelerations, the saccule codes primarily for vertical accelerations, and both organs code for accelerations in the anteroposterior plane. The hair cells of these organs are arranged across the surface of an area called the macula. Near the centre of the macula lies the striola, which separates the macular surface into two parts. The orientation of the utricle has the kinocilium pointing toward the striola, while the saccule has the kinocilium pointing away from the striola. Similar to the semicircular canals, the cilia of the hair cells extend into endolymphatic space and are embedded in a gelatinous membrane. The membrane contains calcium particles called

otoconia. Linear accelerations of the head move the bony structures of the otoliths, but the gravito-inertial forces applied on the otoconia cause the hair cells to deflect in the opposite direction to the movement. Because the orientations of the hair cells on either side of the macula are mirror opposites of each other, a single acceleration will provide two different neural signals as one side of the macula will depolarize (stimulation) and the other side of the macula will hyperpolarize (inhibition).

The neural pathway between the vestibular apparatus and the lower limbs is likely an indirect route (Figure 10). Hair cells are stimulated through a head acceleration and the physical perturbation is transduced into a neural impulse. Primary vestibular neurons, which are part of cranial nerve VIII (vestibulocochlear), carry the impulse to the four vestibular nuclei of the brain stem. The vestibular nuclei are located in the medulla and pons. At this location, vestibular pathways generated from both sides of the head converge and are integrated with additional input from the cerebellum, visual systems, and the reticular formation (Wilson and Peterson 1981; Kiernan and Barr 1998). The lateral vestibular nucleus (Dieter's nucleus) is primarily responsible for neural signals sent down the lateral vestibulospinal tract which extends to interneurons in lumbosacral region of the spinal cord. The final component of this vestibulo-myogenic pathway connects the spinal cord interneurons with alpha and gamma motoneurons that project the neural impulse to muscle fibres in the lower limbs.

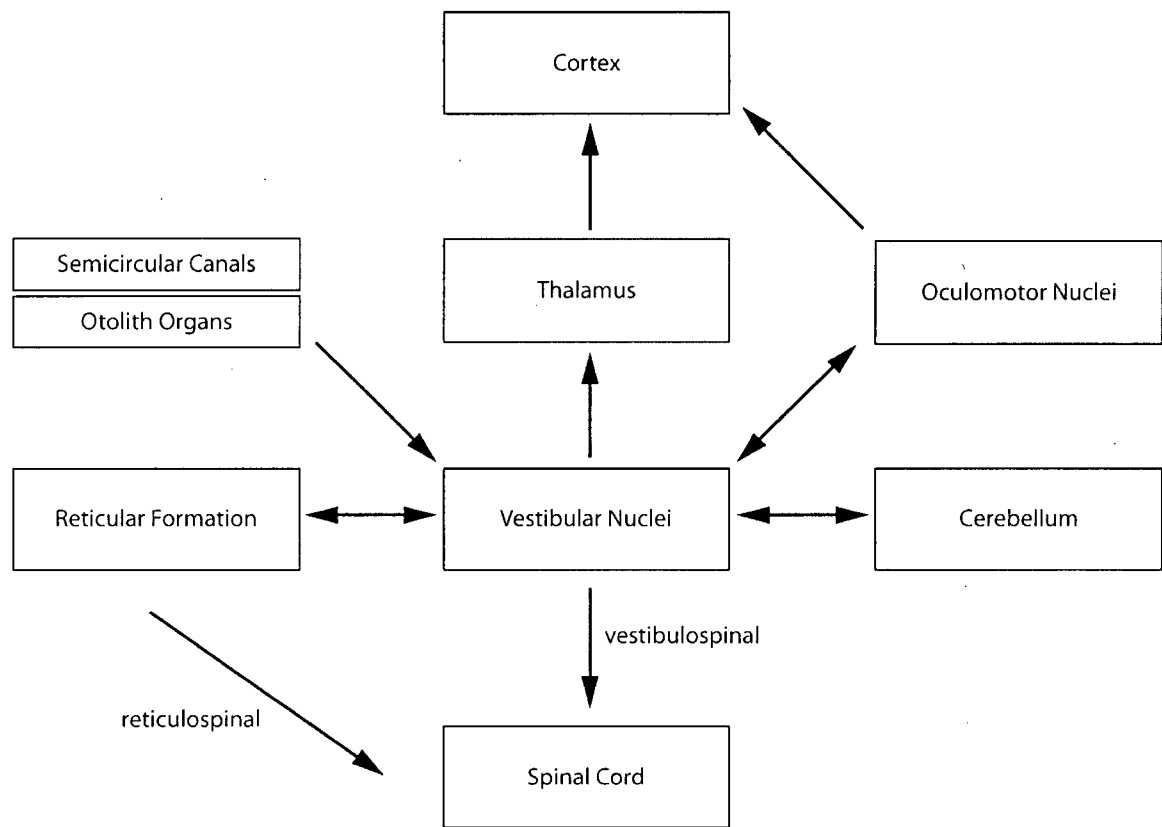


Figure 10. Schematic figure of pathways interacting with the vestibular nuclei that result in the descending vestibulospinal tract that project toward the lower limbs. Note that some connections and structures have been omitted.

Galvanic Vestibular Stimulation

Galvanic vestibular stimulation is a research tool commonly used to probe the vestibular system in humans. This tool has become popular due to its simplicity and ease of use in posture and gait experimental paradigms. A percutaneous current is applied over the mastoid processes. The stimulus bypasses the mechanical perturbation stage and affects the vestibular apparatus at the neuronal level (Speigal and Scala 1943; Pfaltz and Koike 1968; Goldberg et al. 1984). GVS can be applied in many different configurations: bipolar, unipolar, binaural, monoaural, sinusoidal, square-wave, stochastic, or pseudo-random. A common configuration for experiments investigating posture is bipolar,

binaural GVS. With this configuration, an anodal current is applied over one mastoid, while a cathodal current is applied over the other mastoid. The resultant is a virtual head movement as described by the GVS vector model (Fitzpatrick and Day 2004) which cannot be replicated by any naturally occurring kinetic movement.

Vestibular afferents are categorized into two main functional groups according to their background discharge rate: regular and irregular firing afferents (Fernandez and Goldberg 1971). The determinant of regularity is dependent on the amplitude of the afterhyperpolarization relative to the size and rate of the neuron's EPSP (Fitzpatrick and Day 2004). Regular vestibular afferents have strong connections to the spinal cord and oculomotor nuclei, whereas irregular vestibular afferents have strong connections to the supraspinal structures of the CNS (Fitzpatrick and Day 2004). The majority of the vestibular afferents are regular firing and these neurons are only slightly affected by GVS. In contrast, irregular firing vestibular afferents are greatly responsive to galvanic perturbations.

Galvanic vestibular stimulation affects whole-body movements, vestibulo-ocular reflexes, and vestibulo-myogenic reflexes. During quiet stance, GVS (bipolar, binaural configuration) induced sway towards the anode (Lund and Broberg 1983; Pastor et al. 1993), and during forward walking with the eyes closed, GVS induced deviations towards the direction of the anode (Fitzpatrick et al. 1999; Kennedy et al. 2003; Bent et al. 2004a; Bent et al. 2004b; Carlsen et al. 2005). Vestibulo-ocular reflexes are produced when GVS is applied. A torsional oculomotor response occurred with a latency of 46 msec towards the side of the anode (Séverac Cauquil et al. 2003). GVS-evoked muscle responses are present in the upper and lower limbs. A biphasic response was present in

triceps brachii with onset latencies of 41 and 138 msec (Britton et al. 1993) and biphasic responses were present in lower limb muscles (soleus and tibialis anterior) with onset latencies of 58–61 and 94–98 msec (Lee Son et al. 2005).

GVS Vector Model

In a 2004 review by Fitzpatrick and Day, they described a model examining the effects of bipolar, binaural GVS to the vestibular system. The model is explained with the anode over the right mastoid and the cathode over the left mastoid. When a small current is applied, afferents of the right vestibular apparatus will hyperpolarize which will decrease the firing rates of vestibular neurons; afferents of the left vestibular apparatus will depolarize which will increase the firing rates of vestibular neurons. Although head movements can produce similar results in the semicircular canals, GVS stimulation is different from natural kinetic perturbations because GVS-evoked otolithic afferents produce a uniform firing rate on both sides of the striola.

The afferents from the semicircular canals produce a uniform increase or decrease in firing rate depending on the GVS electrode. The modulated firing rate from the horizontal canals are similar to the natural movement code of yaw toward the side of the cathode. GVS modulates the firing rates of the anterior and posterior canals similar to natural movement code of roll toward the side of the cathode. Due to the orientation of the anterior and posterior canals, the effects of pitch are cancelled out and no illusionary pitch movement is created. Vector summation from each vestibular apparatus results in a single vector pointing in a posterior and slightly lateral direction. Since the summated vector is present on both sides of the head, the lateral components are cancelled out when

the two sides are combined. Summation of the two vectors from both sides of the head produces a single vector pointing backwards with respect to the head and slightly upwards with respect to Reid's stereotactic line. The GVS vector produces illusionary head movements of roll and yaw in the direction of the cathode. Therefore, reactive whole-body responses seen through eye movements, postural movements, and centre of pressure are in the direction of the anode.

Otolithic responses to GVS are unlike naturally occurring kinetic perturbations. Natural head movements cause hair cells on either side of the striola to undergo opposite responses, i.e. pars medialis (medial half of the utricle) will depolarize and pars lateralis (lateral half of the utricle) will hyperpolarize. Therefore, for natural movements, each half of the otolith organ will code independently from each other. Using the same GVS configuration for the otoliths as the semicircular canals, all afferents from the right vestibular apparatus will hyperpolarize and all afferents from the left vestibular apparatus will depolarize. The illusionary linear acceleration created from hair cells on one side of the striola will contrast the illusionary linear acceleration created from hair cells on the opposite side of the striola. Each otolith organ will cancel out the sensations associated with afferent hyperpolarization and depolarization within the same otolith organ. Therefore, GVS generates no illusionary movements detected by the otolith organs and hence no responsive postural movement.

GVS-Evoked Muscle Responses

Lower limb muscle responses generated from vestibular perturbations have been extensively studied in humans. When low level stimulation is applied to the mastoid

processes, transient electromyography responses are recorded in the soleus muscle during quiet stance (Nashner and Wolfson 1974; Tokita et al. 1989). The exact neural pathway between vestibular afferents and motoneuron pools in the lower limbs is unclear, but an indirect route is likely. Regular firing vestibular afferents have more direct connections to the spinal cord, while the GVS susceptible irregular firing vestibular afferents have more indirect connections to the spinal cord (Fitzpatrick and Day 2004). Ia presynaptic and Ib inhibitory pathways elicited from peripheral afferent receptors are potential candidates that integrate with the descending vestibular volley before the signal is received at the motor neuron level (Iles and Pisini 1992; Kennedy and Inglis 2001). These interactions are most likely to occur at the spinal cord interneuron level between the somatosensory afferents from the lower limbs that are activated by the postural task and the GVS-evoked vestibular volley. This hypothesis is supported by Marsden et al (2002, 2003) who observed modulations in lateral ground reaction forces elicited by GVS perturbations created by changes in limb loading. These authors argued that somatosensory receptors (from skin, muscle, tendon, or joint) contributed to the load-related changes in the GVS-evoked responses.

Individual responses of the peripheral muscles from GVS pulses are not visible in raw EMG. The reported GVS-evoked muscle responses are shown from rectified, trigger-averaged EMG, typically from soleus or gastrocnemius. Soleus and gastrocnemius are posterior calf muscles that attach to the soleal line of the tibia and fibula (soleus) or medial and lateral condyles of the femur (gastrocnemius) and insert into the Achilles tendon (Tortora and Grabowski 2003). Both muscles contribute to similar movements of plantar flexion about the ankle joint, but in contrast, their muscle fibre compositions are

significantly different. Soleus contains 70% slow-twitch muscle fibres and 30% fast-twitch muscle fibres, whereas gastrocnemius contains 50% slow- and fast-twitch muscle fibres (Edgerton et al. 1975). GVS produces postural responses along the interaural line and toward the side of the anode (Pastor et al. 1993). Therefore, for most GVS-muscle response paradigms, subjects are asked to turn their heads over one shoulder. This experimental setup ensures that the direction of the GVS-evoked sway is in the anteroposterior axis and is aligned with the line of action of the recorded muscles, i.e. soleus. With the head turned to the side and eyes closed, short duration (40 msec), large amplitude (4 mA) GVS perturbations modulated lower limb muscle activities (Figure 11). A biphasic soleus response was reported with a short latency response of 52-60 msec and a medium latency response of 116-124 msec (Britton et al. 1993; Fitzpatrick et al. 1994; Lee Son et al. 2005). Since the initial discovery of the GVS-evoked muscle response, various sensory integration paradigms have been investigated. When subjects opened their eyes, touched a support with their eyes closed, or sat with their eyes closed, the amplitude of the response diminished (Britton et al. 1993). In addition, Britton et al. (1993) observed that the duration and amplitude of the response greatly decreased when the duration of the GVS perturbation decreased.

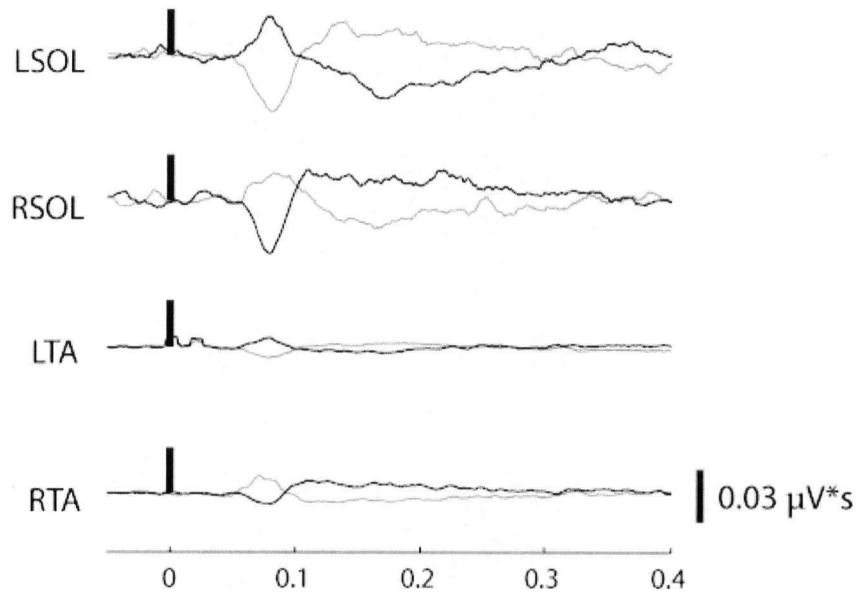


Figure 11. Trigger-averaged left soleus (LSOL), right soleus (RSOL), left tibialis anterior (LTA), and right tibialis anterior (RTA) muscle responses from 20 msec, 4 mA GVS stimulation (Lee Son et al. 2005). GVS polarity was applied randomly with the gray traces having the anode right / cathode left configuration and the black traces having the cathode right / anode left configuration.

Similar to the Britton et al. (1993) study, Fitzpatrick et al. (1994) observed GVS-evoked biphasic muscle responses in soleus with similar onset latencies. In addition, responses were present in tibialis anterior when the muscle was biased by subjects standing on an inclined platform to facilitate tonic activation. Fitzpatrick et al. (1994) modulated the amplitude of the GVS current. They observed an increase in peak-to-peak amplitude when the GVS current was increased. Since Fitzpatrick et al. (1994), many researchers have investigated the GVS-evoked muscle response in various paradigms that included different postural tasks, relationships to biomechanical responses, and their involvement in neurophysiological pathways.

GVS-evoked muscle responses were investigated in the lower limbs with the subjects' heads turned, subjects slightly leaning forward, and eyes closed (Watson and

Colebatch 1998; Welgampola and Colebatch 2001; Rosengren and Colebatch 2002; Welgampola and Colebatch 2002; Ali et al. 2003; Bacsı and Colebatch 2003; Bacsı et al. 2003; Watson et al. 2003; Jankelowitz and Colebatch 2004; Bacsı and Colebatch 2005). The postural parameters: head turned, slightly leaning forward, and eyes closed, were set to maximize the amplitude of the GVS-evoked muscle response. The responses in the soleus and tibialis anterior muscles were also present in the head facing forward and eyes open condition (Lee Son et al., 2005). Although the GVS-evoked muscle responses retain their general shape, modulations to the duration and amplitude of the response were possible under certain conditions. Britton et al. (1993) and Fitzpatrick et al. (1994) observed changes when the duration and amplitude of the GVS current was varied. Additionally, Lee Son et al. (2005) observed that an increase in background EMG increased the size of the response (Figure 12) and that position of the CoM modulated response amplitude (Figure 13).

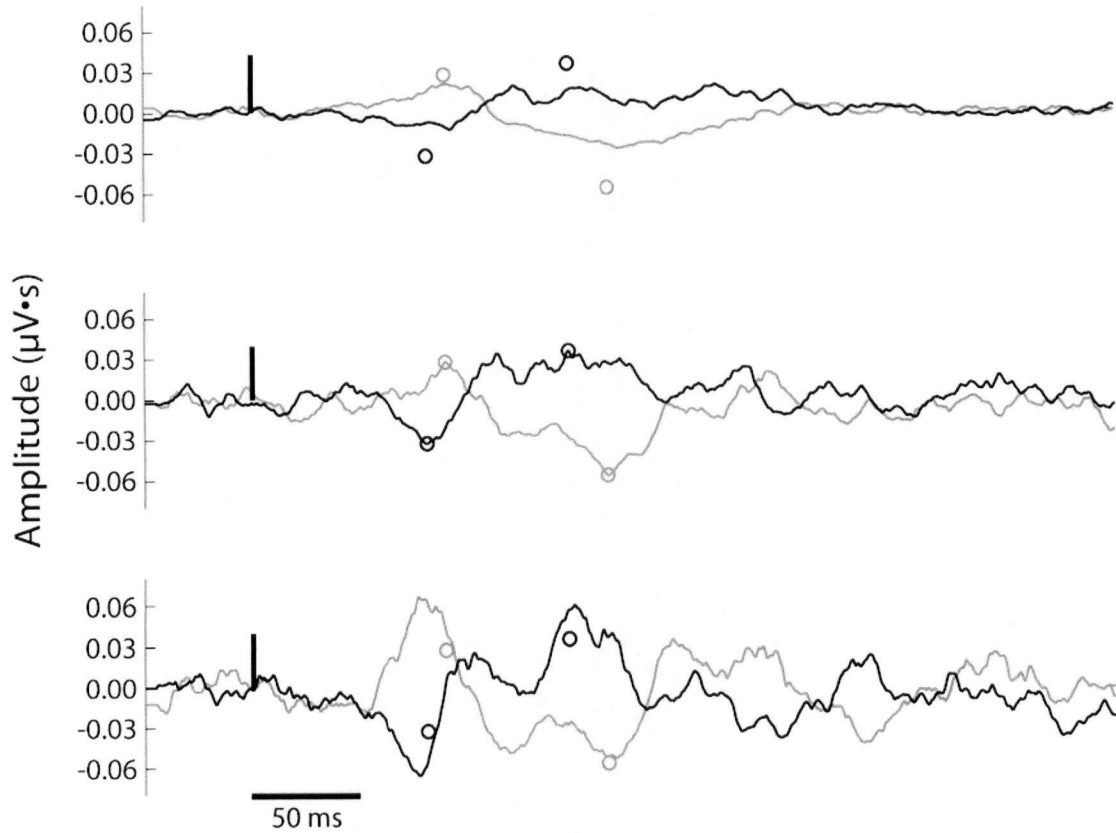


Figure 12. Right soleus muscle responses that are trigger-averaged to the onset of the GVS pulse (Lee Son et al. 2005). The grey traces are responses from the GVS anode right configuration and the black traces are responses from the GVS cathode right configuration. The vertical solid bar represents the onset of the GVS perturbation (4 mA, 20 msec). The top traces represent the muscle responses when background EMGs were minimal. The middle traces represent the muscle responses when background EMGs were median. The bottom traces represent the muscle response when background EMGs were maximal. The circles represent the peak amplitudes of the first and second muscle responses observed for the middle traces. The locations of the circles are superimposed on the responses present in the top and bottom traces.

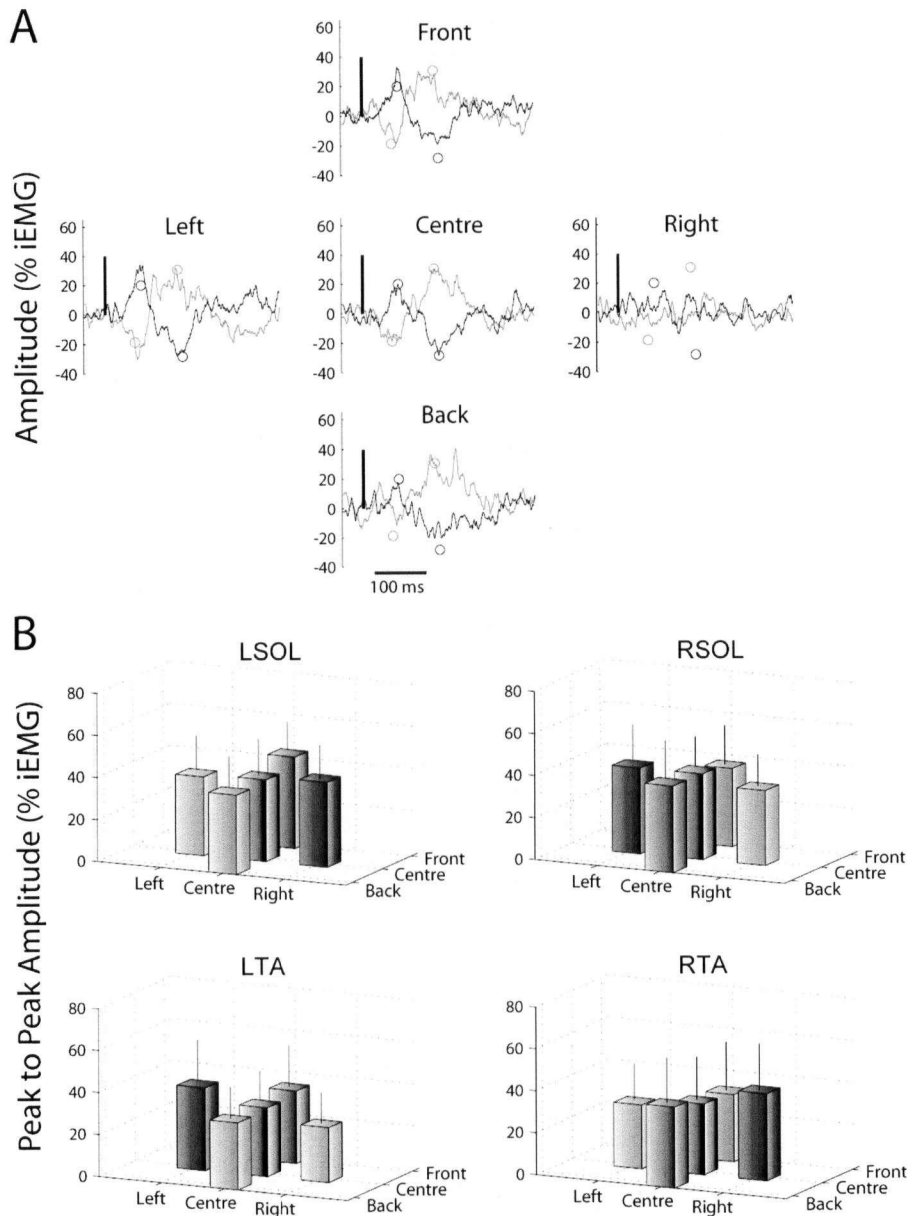


Figure 13. A: GVS-evoked muscle responses ($n=60$ per condition) from the right tibialis anterior that has been normalized for integrated background EMG (iEMG) and sorted by centre of mass (CoM) from a single subject (Lee Son et al. 2005). The grey traces are responses from the GVS anode right configuration and the black traces are responses from the GVS cathode right configuration. The vertical solid bar represents the onset of the GVS perturbation (4 mA, 20 msec). The circles represent the peak amplitudes of the muscle response seen in the centre CoM position. The locations of the circles are superimposed on the responses present for the left, right, front, and back CoM positions. B: Grand mean ($n=12$) of the peak-to-peak amplitudes from right soleus (RSOL), left soleus (LSOL), right tibialis anterior (RTA), and left tibialis anterior (LTA) for all subjects in the specified CoM positions. The vertical lines represent one SD away from the mean value. The three shades of grey represent the CoM positions with the smallest (lightest) to largest (darkest) peak-to-peak amplitudes.

Multiple variations of the GVS standing paradigm have shown modulations in the responses recorded from the lower limb muscles. Two possible explanations for this phenomenon are based on compartmentalization of the muscles or preferential motor unit activation from GVS within the motoneuron pool. Since previous studies have used surface electrodes to record GVS-evoked muscle responses, it is not possible to exclude the neuromuscular compartmentalization hypothesis. Previous studies have shown differential responses in neuromuscular compartments in the lower limbs from external perturbations. For example, the lateral gastrocnemius muscle has three distinct compartments that respond differently to specified body perturbations (Wolf et al. 1998). In the sartorius muscle, there are multiple low-threshold motor units that do not have synchronized contractile activity along the whole length of the muscle (Harris et al. 2005). The other possible explanation for the modulations seen in GVS-evoked muscle responses is differential preference for the type of motor unit within the motoneuron pool. In the cat, vestibular stimulation to the lateral vestibular nucleus influenced the activity of the triceps surae motoneuron pool with a preference toward fast to fatigue motor units (Westcott et al. 1995). In a study done to investigate the effects of GVS on neck muscles, Colebatch and Rothwell (2004) reported that following GVS, the probability of activation decreases for specific motor units at approximately 10 msec after the perturbation. The importance of this study was that it demonstrated that the responses were only apparent when the magnitude (current) of GVS was sufficiently large. It is possible that only high-threshold motor units were susceptible to vestibular input, such that the results were only seen when the current was large enough to activate them (5 mA, 2 msec). These results support the hypothesis that motor unit types do not respond uniformly to

vestibular input and motor unit activation from vestibular input is dependant on the magnitude of the perturbation.

Motor Units

Charles Sherrington coined the term “motor unit” which refers to the cell body and dendrites of a motor neuron, the branches of its axon, and the muscle fibres it innervates (Enoka 2002). Motor units are the functional component in the efferent motor system (Loeb and Ghez 2000) and activation of motor units allows humans to produce graded muscle forces to create body movements. All muscles contain many motor units, each generating small amounts of force during a muscle contraction. Motor units can be classified into three types based on unfused tetanus and their resistance to fatigue: type S (slow), type FR (fatigue resistant), and type FF (fast fatigable) (Rothwell 1994). Type S are slow contracting, fatigue resistant motor units, type FR are fast contracting, fatigue resistant motor units, and type FF are fast contracting, fast to fatigue motor units. Previous research in the cat describes these motor units and their relationship to force production, where type S motor units produce the least amount of force and type FF motor units produce the greatest amount of force (Burke 1981).

Henneman’s size principle of orderly recruitment describes activation of motor units based on the size of the neuron’s cell body (Henneman and Mendell 1981). Henneman evoked a stretch reflex and documented the order of motor unit activation based on action potential amplitude. Action potential amplitude depends on axon diameter which has a positive correlation with cell body size. Therefore, he concluded that motor units were activated in order of increasing size: from the smallest to the largest

motor unit (Enoka, 2002). For a muscle contraction, motor units with small cell bodies are activated initially to generate small amounts of force. As more force is required for the contraction, existing active motor units will increase their frequency of firing (temporal summation). In addition to temporal summation, recruitment of other motor units will occur (spatial summation) to generate more force. The size principle underlies the process with which motor units are recruited. For example, high-threshold motor units are activated last because of the high force output they generate. Therefore, summation of the forces created by these motor units at the peak of contraction will have an effect on the net force, whereas recruitment of low-threshold, low force producing motor units will not have an effect on the net force.

Motor units can be recorded using intramuscular wire electrodes. Classification of motor units can be done during static tasks, such as force ramps (Figure 14). Subjects are asked to increase force or torque production to a specific intensity, while recording intramuscular wire EMG. Identification of the onset of motor unit recruitment with respect to force output provides a estimate of motor unit type. Another motor unit classification technique is to trigger-average the force or moment to the onset of the motor unit firing (Rothwell 1994). Lower threshold, type S motor units will produce longer duration and smaller force output profiles compared to the higher threshold, type FF motor units. An indirect method for motor unit classification is to trigger-average the surface EMG to the onset of the motor unit firing. The resultant is referred to as motor unit triggered-average (MUTA)(Lemon et al. 1990; Jones et al. 1994). Based off the theory of orderly recruitment, higher threshold motor units will only be recruited during times of large force output. Large force output can be associated with large amounts of surface

EMG. Therefore, higher threshold motor units are associated with large surface EMG activity, and thus their MUTAs will possess larger integrated EMG and peak-to-peak amplitudes (Figure 15).

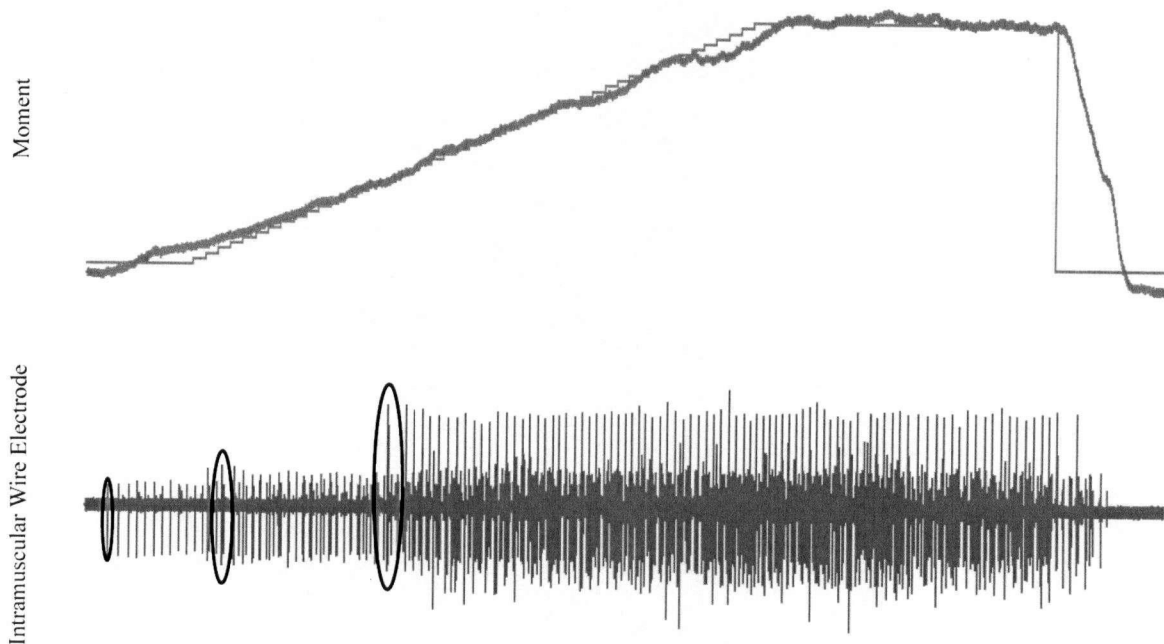


Figure 14. Motor units recruited from the right soleus muscle using an intramuscular wire electrode. The top trace represents a step-wise increase to 20% maximum voluntary contraction and a superimposed trace of the actual moment created by the subject. The bottom trace represents three distinct motor units recruited at different moments around the mediolateral axis generated by plantar flexion against a solid surface.

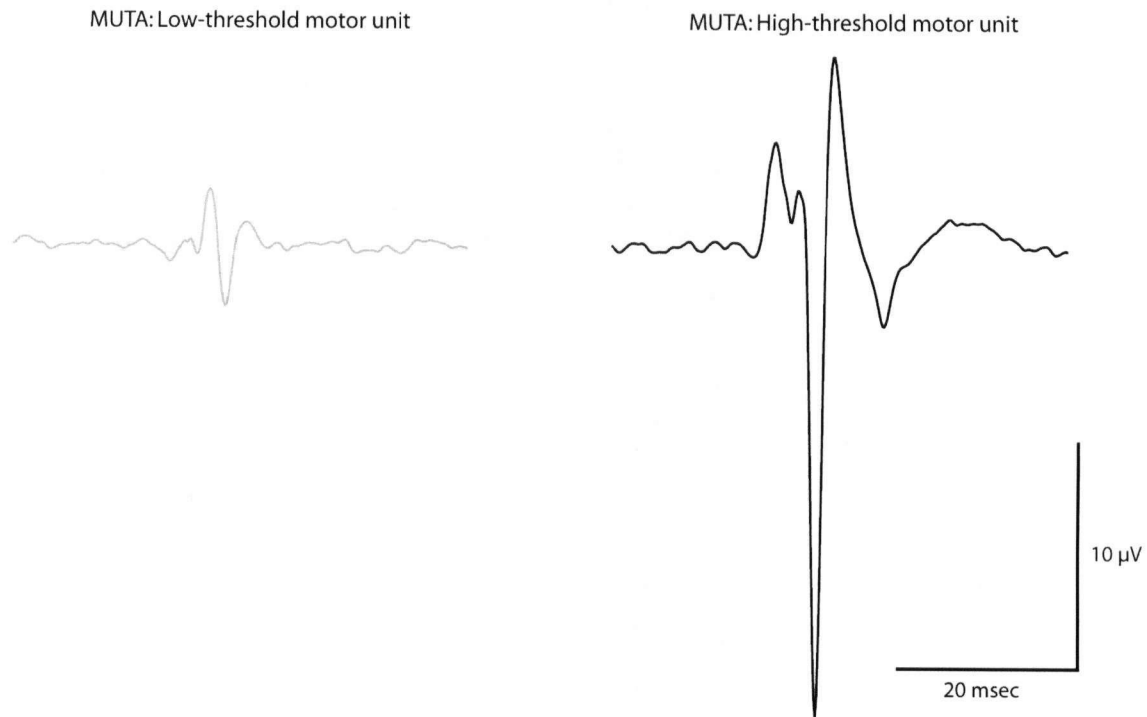


Figure 15. Trigger-averaged surface EMG from the onset of the motor unit firing (MUTA). The left MUTA is associated with a lower threshold motor unit, while the right MUTA is associated with a higher threshold motor unit.

Intramuscular Wire Electrodes (Figure 16)

Wire electrodes were hand-made using stainless steel fine wire (Stainless Steel 304 H-ML, California Fine Wire Company, Grover Beach, USA). For each individual wire, a two-foot piece of wire was cut and folded in half. A hook connected to a drill was used to twist the wire at the folded end until it was smooth. The wire was then threaded through a precision glide needle (Becton Dickinson 25G 1½, Becton Dickinson and Company, Franklin Lakes, USA). At the non-loophole side, the two wire ends were scraped (approximately two cm length) to remove insulation and soldered to metal pins that were connected to a high impedance device (Grass Model HZP, Grass Technologies, West Warwick, USA; Figure 16). The loophole side was cut at a 90 degree angle to the wire (cross-sectional) and the two ends were bent backwards to create a barbed hook

(Figure 16). The hook ends were cut to create an unequal barb with the longer end equal to ~2 mm in length and the shorter end equal to ~1 mm in length. Each wire electrode with insertion needle was placed in a gas sterilization bag and sent to the UBC Hospital Sterilizing Department before use.

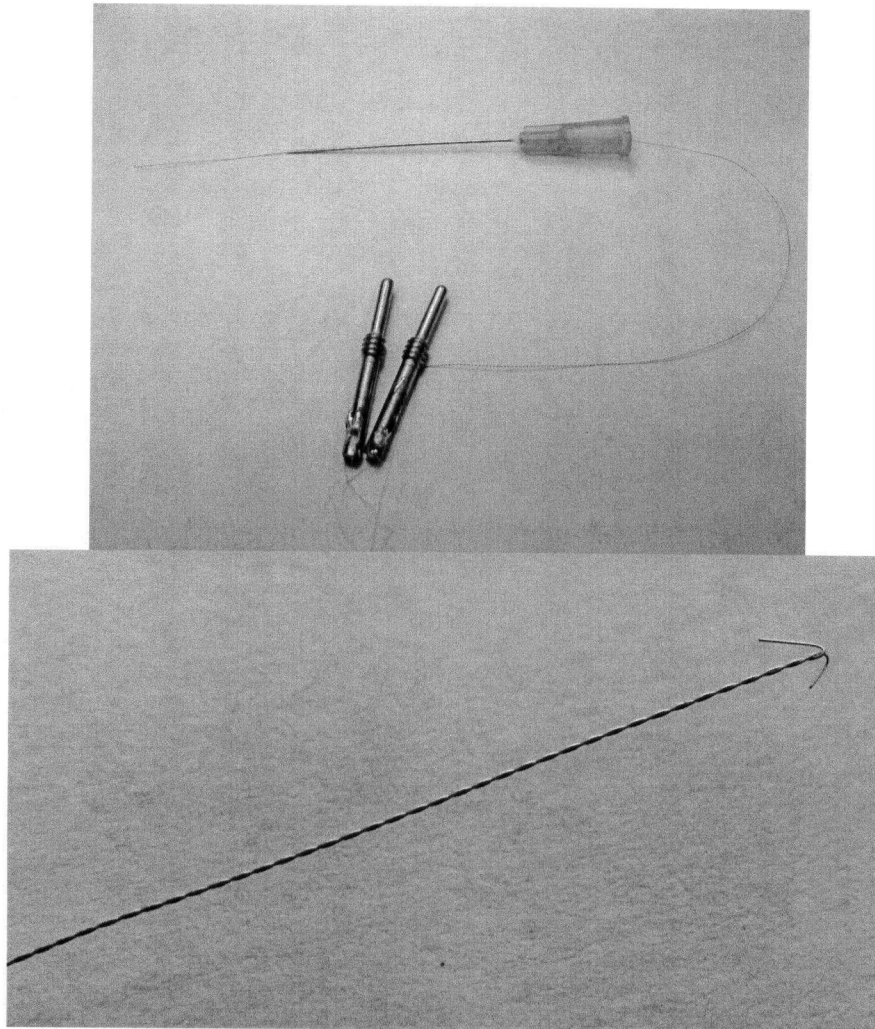


Figure 16. Intramuscular wire electrode. The image on the top shows the complete electrode including wires, insertion needle, and metal pins. The image on the bottom is an up-close view of the barbed tip of the electrode.

During the fine-wire insertion phase, verbal communication between the subject and the experimenter was present to ensure the safety of the subject. The needle/wire

electrode was inserted at the desired location and depth. After the needle/wire electrode had been inserted, the subjects were asked to lightly plantar flex at the ankle joint to recruit soleus motor units. When the position of the electrode was satisfactory to record individual motor units, the needle was rotated 45 degrees and retracted slowly from the muscle. This procedure ensured that the wire was anchored within the muscle. To ensure the safety of the subject and the experimenter, the retracted needle was placed into a safety cannula and taped to the high impedance device. The exposed portion of the wire electrode was taped securely to the subject's leg to prevent further insertion. Upon completion of the experiment, the wire electrode and needle were disposed in a biohazardous sharp container.

Template-Matching

Each wire EMG signal was analyzed using a template-matching algorithm in Spike2 software (Cambridge Electronic Design, Cambridge UK). Individual motor units were identified using the following parameters:

- New Templates*
- Number of similar spikes for a new template.....**8**
- No templates for shapes rarer than 1 in **50** spikes
- Matching a spike to the template*
- Maximum percentage amplitude change for match.....**0**
- Minimum percentage of points in template**60**
- Use minimum percent only when building templates.....**No**

Each identified motor unit was designated to a specific virtual channel and successive occurrences of the same motor unit were classified into the same channel. Verification of the correct motor unit was performed visually through shape recognition. Secondary verification was performed through instantaneous firing frequency analysis.

When instantaneous firing frequency for each motor unit was plotted against time, a bandwidth frequency between 10-20 Hz was expected based on known firing frequencies of motor units. Any motor units that were located outside of the bandwidth was visually inspected and removed from the spike class if the event did not match the motor unit template.

APPENDIX B:

UBC Research Ethics Board Certificate of Approval